Mathematisches Forschungsinstitut Oberwolfach

Report No. 23/2008

# Schnelle Löser für partielle Differentialgleichungen

Organised by
Randolph E. Bank, La Jolla
Wolfgang Hackbusch, Leipzig
Gabriel Wittum, Heidelberg

May 18th – May 24th, 2008

Abstract. The workshop *Schnelle Löser für partielle Differentialgleichungen* (Fast Solvers for Partial Differential Equations), organized by Randolph E. Bank (La Jolla), Wolfgang Hackbusch (Leipzig), and Gabriel Wittum (Heidelberg), was held May 18th–May 23rd, 2008. This meeting was well attended by 41 participants with broad geographic representation from 9 countries (Austria, China, Germany, Israel, Norway, USA, Slovakia, Switzerland, The Netherlands), and 3 continents. The workshop was a nice blend of researchers with various backgrounds.

*Mathematics Subject Classification (2000):* 65N55, 65M55, 65M60, 65N30, 65N50, 65F10, 65F50, 65H10, 65K10.

## Introduction by the Organisers

The conference was organized by Randolph E. Bank, UCSD, La Jolla, Wolfgang Hackbusch, MPI Leipzig, and Gabriel Wittum, University of Heidelberg. This was the fourth one in a series of conferences on fast solvers held at Oberwolfach since 1999. The idea of these workshops is to bring together experts from the different thriving areas of solvers and offer a platform for scientific exchange and progress. The field of solvers for the algebraic systems arising from the discretization of partial differential equations has developed to a major area of numerical mathematics and scientific computing. Solvers are an essential part of simulation codes for problems from science and technology, in many cases determining the complexity of the whole simulation. By virtue of that, the choice of the solver can decide on the reliability of a simulation and if it can be done at all. Thus, solvers are a substantial mathematical component of most simulation tools and a major contribution of mathematics to quite a lot of applied disciplines. This has increased the interest in mathematics of colleagues from the applied sciences over the last

decade substantially.
Major areas of solvers represented at the workshop are: Multigrid methods, H-matrices, domain decomposition methods, and conjugate gradient methods. Often these methods are combined, e.g. multigrid is mostly used as a preconditioner nowadays. Besides that, several talks were given on other aspects of solving partial differential equations, such as discretization schemes and the algebraic properties of the resulting stiffness matrices, overall solution strategies, and application areas where solving plays a crucial role.
The question of the right solver for critical application problems is still open, but new approaches have been developed in recent years. Novel refined approaches like multi-graph-ILU with adaptive choice of elimination thresholds give a new chance of substantially improving the performance. In addition, new lights is shed on the solver question by the recent change of paradigm in computer architecture. The modern multicore processors with additional strong GPU accelerators pose a new and serious challenge for the development of fast solvers. A total of 27 presentations gave a nice overview over the current research, open problems and new developments. Intense discussions provided the opportunity to go into details of novel algorithms and approaches.
In multigrid methods, a lot of research is going in the direction of developing robust methods for special applications. This is a challenging topic requiring mathematical expertise as well as understanding of the model and the application process itself. Another major topic is Algebraic Multigrid. AMG methods are already widespread in several applied communities. However, a lot of open problems remains and the final alforithm is not yet in sight. Several talks also were related to performance issues of multigrid on certain computer architectures such as super scalar or parallel computers. Multigrid research is thriving more than ever.
Another bunch of talks were about domain decomposition methods. These methods are of particular interest for multiphysics problems and parallelization issues. Several new developments have been reported and discussed, giving interesting future perspectives. Often techniques from domain decomposition analysis can be used to analyze other methods e.g. multigrid. A novel technique useful together with domain decomposition and multigrid, but which can also stand on its own, is given by hierarchical matrices (H-matrices). Here, several talks have shown the impressive level of development these methods already have since their introduction in 1998. Further talks have discussed solver techniques for application problems e.g. low Mach-number flow or electromagnetics as well as other problem areas like optimization. Moreover, talks about novel techniques like meshless methods and several other solver techniques have been given.
In total, the workshop was very successfull in bringing together international-level experts from different areas and disciplines. Meanwhile, the Oberwolfach workshop on “Schnelle Löser für partielle Differentialgleichungen” is established as major event in the solver community and a mainstay for novel developments.

## Workshop: Schnelle Löser für partielle Differentialgleichungen

## Table of Contents

# Abstracts

## A generalized regularity result for elliptic PDEs with $L^\infty$ coefficients

Steffen Börm

Let $\Omega \subseteq \mathbb{R}^d$ be an open domain, let $C : \Omega \to \mathbb{R}^{d\times d}$ a mapping satisfying

$$C(x) = C(x)^T, \qquad \alpha I \leq C(x) \leq \beta I \qquad \text{for all } x \in \Omega$$

with $0 < \alpha \leq \beta$. We consider the strongly elliptic partial differential operator

$$\mathcal{L} : H^1_0(\Omega) \to H^{-1}(\Omega), \qquad u \mapsto -\operatorname{div} C \operatorname{grad} u,$$

and aim to solve the equation

$$\mathcal{L}u = f$$

for arbitrary right-hand sides $f \in H^{-1}(\Omega)$.

We discretize the equation by Galerkin's method: for a family $(\varphi_i)_{i\in\mathcal{I}}$ of $H^1_0(\Omega)$-conforming basis functions, we let

$$\Phi : \mathbb{R}^{\mathcal{I}} \to H^1_0(\Omega), \qquad x \mapsto \sum_{i\in\mathcal{I}} x_i \varphi_i,$$

and replace the original equation by

$$Lx = b, \qquad L := \Phi^* \mathcal{L} \Phi, \qquad b := \Phi^* f.$$

The Galerkin approximation of the solution $u$ is given by $u_n := \Phi x$. A major challenge of this approach is finding an efficient solver for the linear system, particularly if the coefficient mapping $C$ is not smooth.

Hierarchical matrix techniques are very successful in this respect. They construct a data-sparse approximation of $L^{-1}$ by choosing subsets $t, s \subseteq \mathcal{I}$ of the index set and replacing the corresponding submatrix $L^{-1}|_{t\times s}$ by a low-rank approximation. The existence of an approximation of $L^{-1}|_{t\times s}$ with rank $k \in \mathbb{N}$ and accuracy $\epsilon \in \mathbb{R}_{>0}$ is equivalent to the existence of a space $W \subseteq \mathbb{R}^t$ of dimension $k$ such that

$$\inf\{\|(L^{-1}y)|_t - z\|_2 \ : \ z \in W\} \leq \epsilon \|y\|_2 \qquad \text{for all } y \in \mathbb{R}^{\mathcal{I}} \text{ with } \operatorname{supp} y \subseteq s.$$

In the continuous setting, this inequality corresponds to

$$\inf\{\|(\mathcal{L}^{-1}g)|_\tau - w\|_{H^1(\tau)} \ : \ w \in \mathcal{W}\} \leq \epsilon \|g\|_{H^{-1}(\Omega)} \qquad \text{for all } g \in H^{-1}(\Omega) \text{ with } \operatorname{supp} g \subseteq \sigma$$

for a $k$-dimensional space $\mathcal{W}$ and pairs $\tau, \sigma \subseteq \Omega$ of subdomains. If the parameters of the problem are analytic, standard interior regularity results imply that $(\mathcal{L}^{-1}g)|_\tau$ is analytic with sufficiently large convergence radius if an *admissibility condition* of the form

$$\operatorname{diam}(\tau) \leq \eta(\tau, \sigma)$$

holds, therefore we can choose $\mathcal{W}$ as the space of polynomials of order $m \in \mathbb{N}$ and get exponential convergence with respect to $m$.

Using the techniques presented in [1], it is possible to prove that an approximating space $\mathcal{W}$ still exists if the problem parameters are no longer analytic, as long as the spectra of the coefficient matrices $C(x)$ are uniformly bounded away from from 0 and $\infty$.

In order to get a similar result for the matrix $L^{-1}$, the original work [1] uses an $L^2$-projection to construct an approximation of $L^{-1}$ from an approximation of $\mathcal{L}^{-1}$. Since the $L^2$-projection is non-local, this approach is not able to provide error estimates for individual blocks.

In order to improve this result, we replace the $L^2$-projection by a Clément-type interpolation operator [3], since its locality properties allow us to find blockwise estimates. We define the operator based on a family $(\lambda_i)_{i\in\mathcal{I}}$ of $L^2$-continuous functionals satisfying

$$\begin{aligned}
\operatorname{supp}\lambda_i &\subseteq \operatorname{supp}\varphi_i && \text{for all } i\in\mathcal{I}, && \text{(locality)}\\
\lambda_i(\varphi_j) &= \delta_{ij} && \text{for all } i,j\in\mathcal{I}, && \text{(projection)}\\
\|\lambda_i(u)\varphi_i\|_{L^2(\Omega)} &\lesssim \|u\|_{L^2(\operatorname{supp}\varphi_i)} && \text{for all } i\in\mathcal{I}, u\in L^2(\Omega). && \text{(stability)}
\end{aligned}$$

Using these functionals, an intermediate operator

$$\Lambda : L^2(\Omega)\to\mathbb{R}^{\mathcal{I}}, \qquad\qquad u\mapsto(\lambda_i(u))_{i\in\mathcal{I}}$$

can be defined, and $\mathfrak{I} := \Phi\Lambda$ is a Clément-type interpolation operator. The matrix

$$S := \Lambda\mathcal{L}^{-1}\Lambda^*$$

provides a second approximation of $u$ in the discrete space: we have

$$\tilde{u}_n := \Phi S b = \Phi\Lambda\mathcal{L}^{-1}\Lambda^*\Phi^* f = \mathfrak{I}\mathcal{L}^{-1}\mathfrak{I}^* f.$$

Using the projection property and $L^2$-stability of $\mathfrak{I}$, we can prove

$$\|u_n-\tilde{u}_n\|_{L^2(\Omega)} \lesssim \|u_n-u\|_{L^2(\Omega)},$$

therefore $\tilde{u}_n$ will converge to $u_n$ at a rate that is consistent with the rate of the $L^2$-norm convergence.

This means that we can restrict our attention to approximating the matrix $S$ instead of the inverse $L^{-1}$. Since the mapping $\Lambda$ defining $S$ is *local*, the approximation estimates for $\mathcal{L}^{-1}$ carry over directly to discrete counterparts for $S$, and we can conclude that $S$, and therefore also $L^{-1}$, can be approximated by hierarchical matrices.

Using the general theory presented in [2], we can prove that $S$ can also be approximated by $\mathcal{H}^2$-matrices. Numerical experiments indicate that this approach is particularly efficient for large problem dimensions.

## References


[1] M. Bebendorf and W. Hackbusch, *Existence of $\mathcal{H}$-matrix approximants to the inverse FE-matrix of elliptic operators with $L^\infty$-coefficients*, Numerische Mathematik, 95:1–28, 2003.

[2] S. Börm, *Data-sparse approximation of non-local operators by $\mathcal{H}^2$-matrices*, Linear Algebra and its Applications, 422:380–403, 2007.

[3] P. Clément, *Approximation by finite element functions using local regularization*, RAIRO Anal. Numér., 9:77–84, 1975.

## Reliable a posteriori error estimates without generic constants

Dietrich Braess
(joint work with Joachim Schöberl)

The talk is concerned with a posteriori error estimates for finite element solutions of elliptic differential equations. Specifically we want upper estimates that have no generic constant in the main term. It turns out that we obtain in this way also a priori error estimates which are not known from classical finite element theory. Moreover for the *hp* method, the asymptotic behavior of the new estimator is better than that of residual estimators.

For convenience, we restrict ourselves to the Poisson equation in a two-dimensional domain $\Omega$,

$$\begin{aligned} -\Delta u &= f \quad \text{in } \Omega, \\ u &= 0 \quad \text{on } \partial\Omega \end{aligned} \tag{1}$$

and to linear elements on a partition $\mathcal{T}_h$ of $\Omega$ into triangles. Here the mixed method for the Poisson equation will also be important, i.e., the system $\sigma = \nabla u$, $\operatorname{div}\sigma = -f$. A flux $\sigma$ which satisfies the second equation is called *equilibrated*. The point of departure is the following theorem [14]. $\Gamma_D$ and $\Gamma_N$ are the parts of the boundary with Dirichlet and Neumann boundary conditions, respectively. All norms without specification are $L_2$ norms.

**Theorem of Prager and Synge (Two-Energies-Principle).**
*Let $\sigma \in H(\operatorname{div})$, $\sigma \cdot n = 0$ on $\Gamma_N$ while $v \in H^1(\Omega)$, $v = 0$ on $\Gamma_D$, and assume that*

$$\operatorname{div}\sigma + f = 0. \tag{2}$$

*Furthermore, let $u$ be the solution of the Poisson equation. Then,*

$$\|\nabla u - \nabla v\|^2 + \|\nabla u - \sigma\|^2 = \|\nabla v - \sigma\|^2. \tag{3}$$

There is much freedom in choosing $v$ and $\sigma$. We also find the name *hypercircle method* in connection with the theorem. We emphasize that it is not restricted to the Poisson equation. We will refer at the end of this abstract to some other elliptic problems for which there are also theorems of Prager–Synge type.

Let $v = u_h$ be a finite element solution for which an a posteriori error estimate is wanted. The crucial step is the construction of an equilibrated flux $\sigma$. In contrast to Neittaanmäki and Repin [12] we perform the construction by computing a correction $\sigma^\Delta := \sigma - \nabla u_h$ to the given gradient of $u_h$, i.e., we use the information that we have a finite element solution.

Following [8] the computation will be performed within the *broken Raviart–Thomas space* of lowest order

$$\mathcal{RT}_{-1} := \{\tau \in L_2(\Omega);\ \tau|_T = a_T + b_T x,\ a_T \in \mathbb{R}^d,\ b_T \in \mathbb{R}\ \forall T\},$$

and the triangulation is the same as that for which the finite element solution was computed. The subspace of functions with continuous normal components is the usual space

$$\mathcal{RT}_0 := \mathcal{RT}_{-1} \cap H(\operatorname{div}).$$

Furthermore we denote the space of piecewise constant functions by $\mathcal{M}^0$.

The first step of the construction brings a separation of the *data oscillation*

$$ch\|f - \bar{f}\|.$$

Here, $\bar{f}$ is the $L_2$ projection of the given right-hand side of (1). This term of higher order is found in most a posteriori error estimates.

Now we make an excursion to the mixed method by Raviart–Thomas

$$\begin{aligned} (\sigma_h, \tau) + (\operatorname{div}\tau, w_h) &= 0 && \forall \tau \in \mathcal{RT}_0 \\ (\operatorname{div}\sigma_h, v) &= -(\bar{f}, v) && \forall v \in \mathcal{M}^0. \end{aligned} \tag{4}$$

Note that $\sigma_h$ is a piecewise linear function. Therefore, $\operatorname{div}\sigma_h$ is piecewise constant as well as $\bar{f}$ is by definition. Since we also test with functions in $\mathcal{M}^0$, it follows that

$$\operatorname{div}\sigma_h = -f \tag{5}$$

holds in the classical sense. In particular $\sigma_h$ is equilibrated. It is easy to show that $\sigma_h$ is even the equilibrated function in $\mathcal{RT}_0$ for which $\|\sigma - \nabla u_h\|$ is minimal.

The computation of the solution of (4), however, is considered as too expensive for an a posteriori error estimation. Fortunately there is a cheap local procedure that provides a suitable approximation. It proceeds on patches of the FE-mesh.

Consider a vertex $V$ of the triangulation $\mathcal{T}_h$ and let $\omega_V$ denote the patch of triangles around $V$:

$$\omega_V := \bigcup_{V \in \bar{T}} T\,.$$

The nodal basis function $\varphi_V$ with $\varphi_V(V) = 1$ and support $\omega_V$ is inserted into the finite element equation $\int_{\omega_V} \nabla u_h \cdot \nabla \varphi_V = \int_{\omega_V} f\varphi_V$. By partial integration we see that the left-hand side equals $\sum_{E\subset\omega_V} \int_E [\nabla u_h \cdot n]\varphi_V$. We recall that $\operatorname{div}\sigma = -\bar{f}$ is the aim. Since all factors in the integrals are now piecewise linear or piecewise constant, we conclude that in the 2-dimensional case

$$\frac{1}{2} \sum_{E\subset\omega_V} [\nabla u_h \cdot n]_E\,|E| = \frac{1}{3} \sum_{T\subset\omega_V} \operatorname{div}\sigma_T\,|T|\,. \tag{6}$$

For this reason, we can shift one half of the jumps of $\nabla u_h \cdot n$ to obtain a Raviart–Thomas function $\sigma_{\omega_V}$ with one third of the required divergence in all triangles of the patch. The algorithmic implementation for problems in 2-space has a simple geometric interpretation and is described in [4, p. 181]. Otherwise merely small systems of algebraic equations have to be solved.

By repeating the procedure on all patches $\omega_V$ for all vertices $V$, we encounter each edge twice and each triangle three times. Hence, the sum $\sigma^\Delta := \sum_V \sigma_{\omega_V}$ yields a function $\sigma_h := \nabla u_h + \sigma^\Delta \in \mathcal{RT}_0$ with $\operatorname{div}\sigma_h = -\bar{f}$. Now the theorem of Prager and Synge provides the guaranteed estimate

$$\|\nabla u - \nabla u_h\| \le \|\sigma^\Delta\| + ch\|f - \bar{f}\|\,. \tag{7}$$

This is the required upper estimate. The ingredients in (6) for the construction are just the quantities found in residual estimators. Therefore, (7) is equivalent to the residual estimator, and the new estimator is not only reliable, but also efficient.

The main diffference to other estimates with equilibrated fluxes (e.g., [12]) or with local Neumann problems [2] is our reduction to *finite dimensional* auxiliary problems. The construction on refined meshes, however, is required, e.g., in [9]. We emphasize that the connection between papers on this topic is often not recognized at first glance, if the theorem of Prager and Synge, the hypercircle method, and the two-energies-method are not cited.

It follows from the theorem of Prager and Synge and the efficiency of (7) that we have $\|\sigma_h - \nabla u\| \le c\,\|\nabla u_h - \nabla u\| + ch\|f - \bar{f}\|$. This inequality applies to the solution $\sigma_h$ of the mixed method by Raviart–Thomas. A byproduct is a comparison of different finite element families.

Classical results say that the error of the conforming $P_1$ element $u_h^{(1)}$, of the nonconforming $P_1$ element $u_h^{CR}$, and of the Raviart–Thomas element $\sigma_h^{RT}$, respectively, is $O(h)$. It is not excluded that one method is substantially better than the other ones for a special right-hand side $f_1$, while there is a different preference for some $f_2$. Now we get a more positive information by recalling that we have already used complementary spaces in (7). We also incorporate Ainsworth' application of the hypercircle method [1]. As usual, $A \preceq B$ means $A \le cB$ and $A \approx B$ that $A \preceq B$ and $B \preceq A$ holds.

**Theorem**. Assume that $f$ is piecewise constant on the FE-mesh. Then

$$\|\nabla u_h^{(2)} - \nabla u\| \preceq |\nabla u_h^{CR} - \nabla u\|_{0,h} \approx \|\sigma_h^{RT} - \nabla u\| \preceq \|\nabla u_h^{(1)} - \nabla u\|\,.$$

We will comment on the differences to similar procedures in the literature and note that small changes may have much impact on the computing effort. Moreover, applications to quite different elliptic problems will be listed (without saying how our procedure has to be adapted). Because of the lack of space, we will cite explicitly only one representer of closely related research.

**Remarks.**

1. Melenk and Wohlmuth [10] showed by theoretical and numerical investigations that the efficiency of residual estimators deteriorates as $O(p)$ when applied to the *hp* method. Numerical experiments, however, show efficiency factors not far from $\sqrt{2}$ for the hypercircle method. Indeed, full efficiency could be proven for rectangular grids by the construction of uniformly bounded right inverses of the divergence operator in polynomial spaces, i.e.,

$$\|\sigma_h\|_{L_2} \le c\|f\|_{H^{-1}}\,.$$

The main tool is a suitable interpolation on tensor products [7]. However, we did not succeed in treating triangular meshes.

2. The construction of equilibrated fluxes for the Lamé equation is more involved, since mixed methods for symmetrical stress tensors require a larger number of local degrees [13].

3. The approach of Repin (see, e.g., [12]) is directed to arbitrary approximate functions with respect to the elliptic problem, and the knowlege of the FE solution is not used for the construction. The latter is therefore more expensive.

4. Edge elements and the equations of magnetostatics are easily treated in the framework of the two-energies-principle [8].

5. A theorem of Prager–Synge type can be formulated for variational inequalities as found in obstacle problems or contact problems. An implementation without extra terms, however, is restricted to active sets with some regularity; see, e.g., [6, 15].

6. The two-energies-principle has also been applied on the continuous level in order to justify or discard plate models [3, 11]. Admissible functions for $v$ and $\sigma$ in 3-space are constructed from the solutions in the lower dimensional spaces.

## References


[1] M. Ainsworth, *A posteriori error estimation for lowest order Raviart Thomas mixed finite elements.* Preprint 2007

[2] M. Ainsworth and T.J. Oden, A Posteriori Error Estimation in Finite Element Analysis. Wiley, Chichester 2000.

[3] A.L. Alessandrini, D.N. Arnold, R.S. Falk, and A.L. Madureira, *Derivation and justification of plate models by variational methods.* In "Plates and Shells, Quebec 1996", (M. Fortin, ed.), pp. 1-20. CRM Proceeding and Lecture Notes, vol. 21, American Mathematical Society, Providence, RI 1999.

[4] D. Braess, Finite Elements: Theory, Fast Solvers and Applications in Solid Mechanics. 3rd edition. Cambridge University Press 2007.

[5] D. Braess, *An a posteriori error estimate for the nonconforming $P_1$ element.* (submitted)

[6] D. Braess, R. Hoppe, and J. Schöberl, *A posteriori estimators for obstacle problems by the hypercircle method.* Comp. Visual. Sci. (in press)

[7] D. Braess, V. Pillwein, and J. Schöberl, *Equilibrated residual error estimates are p-robust.* (submitted)

[8] D. Braess and J. Schöberl, *Equilibrated residual error estimator for edge elements.* Math. Comp. 77 (2008), 651–672.

[9] R. Luce and B. Wohlmuth, *A local a posteriori error estimator based on equilibrated fluxes.* SIAM J. Numer. Anal. **42** (2004), 1394–1414.

[10] J.M. Melenk and B.I. Wohlmuth, On residual-based a posteriori error estimation in hp-FEM. Adv. Comput. Math. 15 (2001) 311–331.

[11] D. Morgenstern, *Herleitung der Plattentheorie aus der dreidimensionalen Elastizitätstheorie.* Arch. Ration. Mech. Anal. **4** (1959), 145-152.

[12] P. Neittaanmäki and S. Repin, Reliable Methods for Computer Simulation. Error control and a posteriori estimates. Elsevier. Amsterdam 2004.

[13] S. Nicaise, K. Witowski, and B. Wohlmuth, *An a posteriori error estimator for the Lamé equation based on $H(\mathrm{div})$-conforming stress approximation.* IANS report 2006/005, University of Stuttgart.

[14] W. Prager and J.L. Synge, *Approximations in elasticity based on the concept of function spaces.* Quart. Appl. Math. **5** (1947), 241–269.

[15] A. Weiss and B. Wohlmuth, *A posteriori error estimator and error control for contact problems.* IANS report 12/2007, University of Stuttgart.

## Adaptive Eigenvalue Computation

Wolfgang Dahmen
(joint work with T. Rohwedder, R. Schneider, A. Zeiser)

Given a Gelfand-triple $\mathcal{H} \hookrightarrow \mathcal{X} \hookrightarrow \mathcal{H}$ and a symmetric positive definite norm-isomorphism $\mathcal{L}$ from $\mathcal{H}$ onto its normed dual $\mathcal{H}'$, consider the eigenvalue problem

$$\mathcal{L}u = \lambda \mathcal{E} u, \tag{1}$$

where $\mathcal{E} : \mathcal{H} \to \mathcal{H}'$ is the canonical embedding. In particular, one is interested in finding the eigenpair $(\underline{\lambda}, u)$ where $\underline{\lambda}$ is the smallest eigenvalue which is assumed to be simple and separated from the rest of the spectrum. The typical approach is to discretize (1) and then look for efficient methods for solving the resulting finite dimensional eigenvalue problem. There is a vast amount of literature on problems of this type and a rich supply of tools developed in numerical linear algebra. In this work we deviate from the known approaches in that the discretization and solution process is completely intertwined. In fact, we outline the design and analysis of an adaptive scheme that determines $\underline{\lambda}$ and its corresponding eigensolution $u$ within a given accuracy tolerance at a possibly low computational cost, depending on the regularity of the ground state $u$ [2]. Typical examples that are covered by the approach are $\langle \mathcal{L}u, v\rangle = a(u, v)$ where $a(\cdot, \cdot)$ is a symmetric $H_0^1(\Omega)$-elliptic bilinear form, in which case $\mathcal{H} = H_0^1(\Omega), \mathcal{X} = L_2(\Omega)$, or the stationary Schrödinger operator (with an appropriate spcetral shift). A related adaptive procedure for similar problem classes has recently been proposed also in [4] in a finite element framework which, however, does not give any complexity estimates. In the spirit of [1] the strategy used here relies on transforming the original problem with the aid of a Riesz basis for $\mathcal{H}$ (wavelet bases, hyperbolic wavelet bases, eigenfunctions derived from single particle operators) into an equivalent eigenproblem formulated on $\ell_2$, the space of square summable sequences on the index set stemming from the Riesz basis. In contrast to the situation encountered with standard discretizations, the representation in terms of the Riesz basis can be shown to guarantee the the (infinite dimensional) problem is well conditioned. As a consequence a gradient type iteration for the minimization of Rayleigh quotients on all of $\ell_2$ turns out to exhibit a fixed error reduction rate per step. Some ingredients of the proof are highlighted. It then remains to realize numerically these (ideal) iterations within suitable dynamically updated error tolerances. This is based on the adaptive application of operators so as to compute the relevant quantities in the ideal iteration within properly chosen tolerances at minimal cost. It is shown under which circumstances the resulting adaptive scheme, which can be viewed as a perturbation of the ideal descent scheme on all of $\ell_2$, exhibits in some sense asymptotically optimal complexity when compared with rates of best $N$-term approximation. This can be shown to hold when the matrix representations are compressible in the sense of [1, 3] which is known to be the case for a wide span of operators and wavelet bases. Furthermore, it is indicated how to exploit the fact that in the infinite dimensional (ideal) iteration the accuracy of the Rayleigh quotient corresponding to an approximate eigenvector is essentially the square of

the accuracy of that approximate eigenvector. It is shown that, in principle, this leads to an even improved concergence and complexity order when compared with the $N$-term approximation rate of $u$.

### References

[1] A. Cohen, W. Dahmen, R. DeVore, *Adaptive wavelet methods II - Beyond the elliptic case*, Foundations of Computational Mathematics, **2** (2002), 203–245.
[2] W. Dahmen, T. Rohwedder, R. Schneider, A. Zeiser, Adaptive Eigenvalue Computation - Complexity Estimates, IGPM Report, Nov. 2007, RWTH-Aachen, to appear in Numer. Math.
[3] T. Gantumur, R. Stevenson, Computation of differential operators in wavelet coordinates, Math. Comp., 75(2006), 697–709.
[4] S. Giani, I. Graham, A convergent adaptive method for elliptic eigenvalue problems, BICS Preprint, June 2007, Bath Institute for Complex Systems.

## Parallel Sweeping Algorithms in SN Transport

Robert Falgout

A potential bottleneck when solving Boltzmann transport equations in parallel is the inversion of the streaming operator. The discretized form of this operator is a lower triangular matrix or block lower triangular matrix with small blocks. The solution of these triangular systems by direct methods is inherently sequential. Although various overloading techniques have been used to amortize the costs of these lower triangular solves or "sweeps", the practicality of scaling to massively parallel machines with tens of thousands of processors is unclear.

In this talk, we present new theoretical scaling models for sweeping algorithms and compare with experiment. In theory, these algorithms have the potential to scale like $O(dP^{1/d} + M)$, where $d$ is the spatial dimension of the problem, $M$ is the number of angles, and $P$ is the number of processors. When $M$ is fairly large, it masks the effect of the $P$ term, whereby delaying the poor asymptotic scaling behavior. This delay may be adequate in some cases to get practical performance, even up to tens of thousands of processors. However, some popular parallel sweep algorithms scale worse than this best-case theoretical model. This is also discussed in the talk.

## Flux-based level set method

Peter Frolkovič
(joint work with Karol Mikula and Christian Wehner)

Flux-based level set method is a new finite volume method to solve partial differential equations that describe the movement of all isolines (in 2D case) or isosurfaces (in 3D) of some level set function.

The most common application of such level set equations is an implicit representation of dynamic interfaces that can represent, e.g., the free boundary between different phases in two-phase flows [4], the moving subjective surface in image

segmentation [8], the first arrival time for fire spread [3], and so on. In such applications, the interface is represented by, e.g., the zero level set, and the level set equation is solved on an enlarged fixed domain that contains the moving interface. For a comprehensive review on level set methods we refer to [11, 12].

The most concise form of the level set equation can be given by

$$\partial_t \phi + \vec{v} \cdot \nabla \phi = f \,, \tag{1}$$

where the unknown function $\phi = \phi(x,t)$ is prescribed at $t = 0$ by some initial conditions. The velocity $\vec{v}$ can be defined by some external vector field $\vec{v} = \vec{V}(x)$ and/or by some speed $F$ in normal direction $\vec{N}$ to isolines or isosurfaces. In the latter case one has $\vec{v} = F\vec{N}$ and $\vec{N} = \frac{\nabla\phi}{|\nabla\phi|}$ (if the gradient of $\phi$ is well defined), so (1) turns to

$$\partial_t \phi + F|\nabla\phi| = f \,. \tag{2}$$

Usualy, the right hand side of (1) is zero (i.e., $f \equiv 0$), but for some applications where the stationary solution of (1) is searched, $f$ can be non-zero. The boundary conditions for (1) are not discussed here.

The so called complementary volume discretization scheme for level set like equations was studied in [9] that can be viewed as finite volume method for the equation

$$\partial_t \phi - |\nabla\phi| \nabla \cdot \left( \frac{\nabla\phi}{|\nabla\phi|} \right) = 0 \,. \tag{3}$$

The level set equation (3) describes the movement of all level sets by the normal mean curvature field and can be obtained from (1) by setting $F = -\kappa$, where $\kappa$ denotes the mean curvature and can be computed from $\kappa = \nabla \cdot \vec{N}$. The finite volume method used in [9] is second order accurate, semi-implicit, linear scheme which is unconditionally stable in $L_\infty$ and $W^{1,1}$ sense for arbitrary time step. The main ingredient of the method is integrating (3) over a co-volume and integrating by parts to obtain the flux-based formulation of finite volume method.

In [5] (or in its extended version [6]), this finite volume technique was derived for more general form of (2), where the speed $F$ includes also a constant normal velocity, e.g., $F = \delta$. The idea is to reformulate the non-divergence form of (1) to conservation law with source term

$$\partial_t \phi + \nabla \cdot (\phi \vec{v}) = -\phi \nabla \cdot \vec{v} \tag{4}$$

and to use the finite volume discretization method. By computing $\vec{v} = \delta \nabla\phi / |\nabla\phi|$ from previous time step, the explicit in time, first order accurate, flux-based method of characteristics [1, 2] with recursive flux redistribution was used for (4) with no CFL constraint on the choice of time step. Several examples in 2D and 3D on structured grids for the evolution of curves and surfaces involving topological changes are presented in [6] with a detailed analysis of unconditionally stable behavior of the scheme for large time steps.

In [7], the so called "high-resolution" form of flux-based level set method was derived for advective level set equation (1), i.e., for the case

$$\vec{v} = \vec{V} + \delta\vec{N}. \tag{5}$$

The method is consistent and second order accurate for unstructured grids with the possibility of limiting the scheme locally to first order accuracy if necessary (the "limiter" procedure). The method is explicit in time and fulfills the discrete minimum/maximum principle under some restriction on time step (the CFL constraint). Several popular benchmarks were computed in [7], including the examples of an expanding/shrinking and rotating circle/square, the single vortex example, and the rotation of Zalesak's disk. All examples are provided with a detailed numerical convergence study (the so called experimental order of convergence) and they document, among others, very good "conservation" property of the scheme.

In [3], the high-resolution flux-based level set method was considered on rectangular grids for level set equation (1) with $f \neq 0$ and $\vec{v}$ given by (5). Several well-established techniques for the computation of (reconstructed) gradient were used and compared. In such way, the benchmarks like the rotation of Gaussian function or the single vortex example could be computed with the experimental order of convergence approaching the order 2 sharply from above. Moreover, new benchmark examples for the computation of first arrival time for the fire spread in the presence of wind were studied numerically in details.

Recently, two more advanced applications were solved using flux-based level set method. Firstly, the method was applied for (subjective) surface evolution in image segmentation of 3D biological data, see [8, 10]. Secondly, a two-phase flow problem using level set formulation for the interface between different phases was solved using finite volume method, see [4].

## References


[1] P. Frolkovič. Flux-based method of characteristics for contaminant transport in flowing groundwater. *Computing and Visualization in Science*, 5(2):73–83, 2002.

[2] P. Frolkovič. Flux-based methods of characteristics for transport problems in groundwater flow induced by sources and sinks. In S.M. Hassanizadeh, R.J. Schotting, W.G. Gray, and G.F. Pinder, editors, *Computational Methods in Water Resources 2*, pages 979–986. Elsevier, 2002.

[3] P. Frolkovič and C.Wehner. Flux-based level set method on rectangular grids and computations of first arrival time functions. *Computing and Visualization in Science*, (published online 17.4.2008, DOI 10.1007/s00791-008-0115-z), 2008.

[4] P. Frolkovič, D. Logashenko, and G. Wittum. Flux-based level set method for two-phase flows. In R. Eymard and J.-M. Herard, editors, *Finite Volumes for Complex Applications*, pages 415–422. ISTE and Wiley, 2008.

[5] P. Frolkovič and K. Mikula. Flux-based level set method: A finite volume method for evolving interfaces. Preprint 15, IWR, Universität Heidelberg, September 2003.

[6] P. Frolkovič and K. Mikula. Flux-based level set method: A finite volume method for evolving interfaces. *Applied Numerical Mathematics*, 57(4):436–454, 2007.

[7] P. Frolkovič and K. Mikula. High-resolution flux-based level set method. *SIAM J. Sci. Comp.*, 29(2):579–597, 2007.

[8] P. Frolkovič, K. Mikula, N. Peyrieras, and A. Sarti. A counting number of cells and cell segmentation using advection-diffusion equations. *Kybernetika*, 43(6):817–829, 2007.

[9] A. Handlovičova and K. Mikula. Semi-implicit complementary volume scheme for solving level set like equations in image processing and curve evolution. *Numer. Math.*, 93(4):675–695, 2003.
[10] K. Mikula, N. Peyrieras, M. Remesikova, and A. Sarti. 3d embryogenesis image segmentation by the generalized subjective surface method using the finite volume technique. In R. Eymard and J.-M. Herard, editors, *Finite Volumes for Complex Applications V.*, pages 585–592. ISTE and Wiley, 2008.
[11] S. Osher and R. Fedkiw. *Level Set Methods and Dynamic Implicit Surfaces*. Springer, 2003.
[12] J. Sethian. *Level Set Methods and Fast Marching Methods*. Cambridge University Press, 1999.

## GPU Accelerated Algebraic Multigrid

Gundolf Haase
(joint work with Manfred Liebmann, Gernot Plank)

### 1. Developments in graphics hardware and programming tools

The race for higher and higher clock frequencies hit a physical road block five years ago, forcing the big processor companies to focus on multi–core architectures instead. The main directions the industry is moving right now are: First, the multi–core CPU architecture implemented by Intel, AMD and others with complex deeply pipelined processing cores and a complex multilevel cache hierarchy. Second, the many–core GPU architecture of Nvidia and AMD with hundreds of simple scalar processors with only a small amount of on–chip memory and a very high bandwidth memory interface. The current generation of GPUs deliver 300–400 GFLOPS peak in single precision arithmetic. The next generation GPUs with full IEEE double precision floating point support will be available in the second half of 2008 with similar performance. The high performance scalar processors on the GPU are fed by a very high bandwidth memory interface to the on-board DRAM with up to 75GB/s throughput. This is an order of magnitude faster than on a typical CPU based server.

Before the introduction of the compute unified device architecture (CUDA) by Nvidia, programming GPUs for non–graphics tasks was very difficult and greatly limited. One had to use vertex and pixel shaders to accomplish data manipulation in a stream based architecture. In contrast CUDA is designed for general purpose algorithms to be executed on the GPU. CUDA provides tools and compilers for the C/C++ programming language for easy integration of GPU kernels with existing code. A great variety of algorithms had already be ported to the graphics processing units using CUDA with great success. A recent collection of applications can be found on the CUDA Showcase[1] page.

Results for unstructured sparse matrix operations [5] using a parallel scan based approach are however discouraging, with no advantage over highly tuned CPU based kernels at all. But as we will outline below, these limitations can be overcome with an highly tuned sparse matrix-vector kernel.

[1] http://www.nvidia.com/object/cuda_showcase.html

## 2. Algorithmic view on algebraic multigrid

We want to solve the system of equations

$$K\underline{\mathfrak{u}} = \underline{\mathfrak{f}} \tag{1}$$

for a symmetric, positive definite $N \times N$ Matrix $K$ and a given right hand side $\underline{\mathfrak{f}}$. The sparse matrix $K$ results from a FEM (FDM, FVM) discretization of the underlying second order boundary value problem in 2D or 3D, see [3].

The basic idea of multigrid consists in a sequence of discretizations, respectively matrices $K_q$, such that the high frequency error components will be reduced on the fine discretization $q$ by smoothing and the lower frequency error components will be projected onto the coarser discretization $q-1$ [1]. The algorithm assumes

**Algorithm 1** Multigrid Method: $\underline{\mathfrak{u}}_q \Leftarrow \text{MGM}(\mathsf{K}_q, \underline{\mathfrak{u}}_q, \underline{\mathfrak{f}}_q, q)$

```
if q == 1 := CoarsestLevel then
  u_q ⇐ Solve( K_q · u_q = f_q )                    {solution on the coarsest grid}
else
  for i = 1 step 1 until ν1(q) do
    u_q ⇐ G_q^pre(u_q)                                          {presmoothing}
  end for
  d_q ← f_q − K_q · u_q                                        {defect calculation}
  d_{q−1} ← I_q^{q−1} · d_q                                          {restriction}
  w_{q−1} ← 0                                          {coarse grid initial guess}
  for j = 1 step 1 until γ(q − 1) do
    w_{q−1} ⇐ MGM(K_{q−1}, w_{q−1}, d_{q−1}, q − 1)                  {recurrent call}
  end for
  w_q ← I_{q−1}^q · w_{q−1}                                          {prolongation}
  u_q ← u_q + w_q                                      {coarse grid correction}
  for i = 1 step 1 until ν2(q) do
    u_q ⇐ G_q^post(u_q)                                        {postsmoothing}
  end for
end if
```

that matrices/operators are already defined. If we have access to the finest discretization then the algebraic multigrid (AMG) method can be applied.

The algebraic multigrid method consists of two parts: First, the setup builds a hierarchy of coarser discretizations from the finest one according to the classical approach by Ruge and Stüben [4], which defines intergrid transfer matrices $I_{q-1}^q$, $I_q^{q-1}$ and calculates the coarse matrices $K_{q-1} := I_q^{q-1} K_q I_{q-1}^q$ via the Galerkin approach. Due to the high algorithmic complexity of the setup, this part of AMG has not yet been implemented on the GPU. Second, after the setup a normal multigrid cycle using the automatically generated hierarchy is applied.

We choose Jacobi-iteration as pre- and postsmoothing operators $\mathsf{G}_q^{pre}$ and $\mathsf{G}_q^{post}$. Therein, in the defect calculation as well as in prolongation $I_{q-1}^q$ and in the restriction $I_q^{q-1}$, the sparse matrix-vector-product is the dominating operation. Hence, a fast matrix–vector product on the GPU is key to a fast AMG solver.

## 3. Unstructured matrix operations on the GPU

The implementation of a sparse matrix–vector kernel on the GPU is complicated by several factors: Most important, the GPU requires a very high degree of parallelism to work efficiently. This means that thousands of threads must be executing for a single computational kernel. A single matrix–vector multiplication thus has to be split into thousands of parallel threads. With a matrix $K \in \mathbb{R}^{N\times N}$ stored in compressed row storage format (CRS) and $u, b \in \mathbb{R}^N$ as full vectors, this goal can be achieved by scheduling a thread for every sparse scalar product.

- **CRS Sparse Matrix-Vector Kernel**
  - Schedule a thread for every sparse scalar product!
  - Thread $i$ calculates $u_i = \sum_{j=1}^{N} K_{ij} b_j$

Although this approach gives us enough threads, the performance of this kernel is very poor. Problems and solutions:

- **Non-coalesced memory access!**
  - Rearrange CRS data structure for coalesced access
  - Interleave the sparse matrix rows for at least 16 consecutive rows
  - Holes in the data structure: Not critical! Typical 5-10% increase in storage
- **Random access to $b$ vector!**
  - Use texture unit of the GPU for random access to $b$ vector
  - Texturing is optimized for spacial locality: Small read-only cache

With the implementation of coalesced memory access and using the texture unit for random access to the vector $b$ the GPU kernel delivers outstanding performance.

## 4. Numerical results

First, we consider the matrix-vector product for two sparse test matrices originating from the pressure correction in a premixed flame problem (courtesy of Brenn/Steiner, TU Graz).

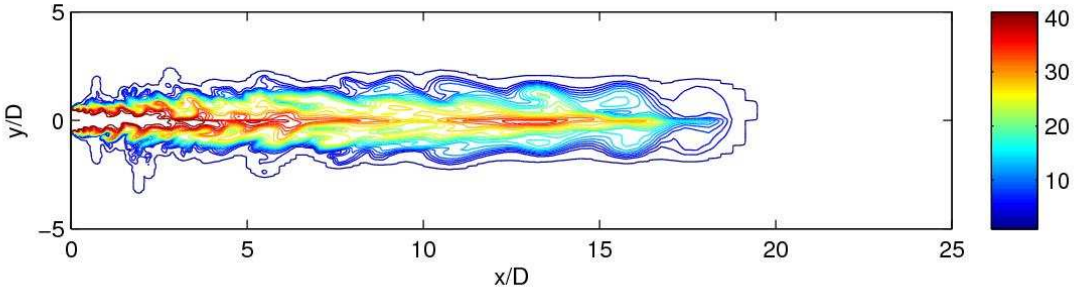

| | N | #A | AMD Opteron 8347 | Intel C2D E6850 | Nvidia Geforce 8800 GT |
|---|---|---|---|---|---|
| (a) | 720,000 | 5,020,800 | 0.25 | 0.97 | 10.1 |
| (b) | 274,625 | 7,189,057 | 0.58 | 1.17 | 10.8 |

TABLE 1. Performance of sparse matrix-vector multiplication in GFLOPS

The benchmark results in table 1 show an order of magnitude performance advantage for the Nvidia Geforce 8800GT GPU over a high–end Intel workstation and a factor 20–40 compared with an AMD Opteron server. All benchmarks use single precision arithmetics to make the comparison fair.

Furthermore, the sparse matrix-vector kernel is used to implement prolongation and restriction operators and the Jacobi-smoothers together with several routines for vector addition and scaling to give the full AMG muligrid cycle on the GPU. We applied the AMG solver as a preconditioner in a preconditioned conjugate gradient (PCG) algorithm to solve the pressure equation from above [(a) and (b)] and to solve the potential problems occurring in the simulation of the electrical activity in a rabbit heart [(c) and (d)].

| | $N$ | $\#A$ | Intel E6850 | Nvidia 8800 GT |
|---|---|---|---|---|
| (a) | 720.000 | 5,020.800 | 0.089777 | 0.0122688 |
| (b) | 274.625 | 7,189.057 | 0.050223 | 0.0078146 |
| (c) | 862.515 | 12,795.209 | 0.158694 | 0.0219833 |
| (d) | 111.589 | 1,445.373 | 0.017278 | 0.0038916 |

TABLE 2. Timing of PCG-AMG iteration in seconds

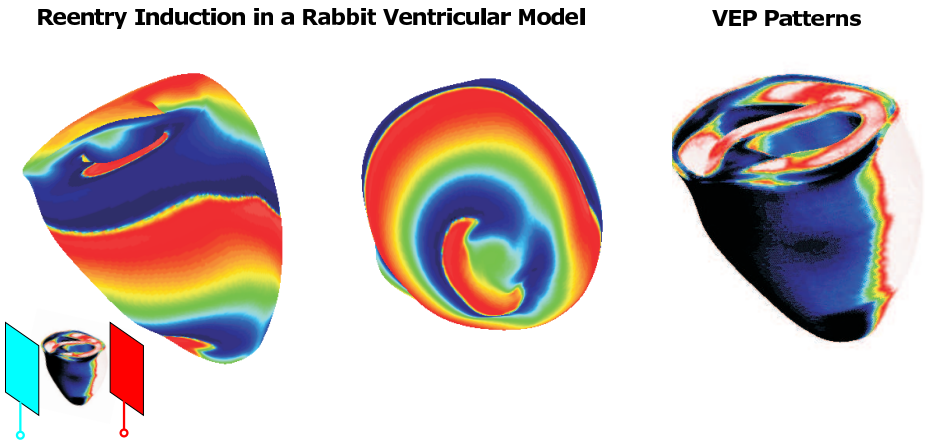


The PCG-AMG benchmark for solving the system of equations 1 shows that the GPU version is 6–8 times faster compared with a high-end Intel C2D E6850 3.0Ghz workstation running the highly optimized implementation of the Parallel Toolbox[2]. For the AMD Opteron 8347 1.9 GHz machine the performance differential is even

[2]http://paralleltoolbox.sourceforge.net

wider, giving the GPU a 16–24 fold advantage. All benchmarks used single precision arithmetics.

## 5. Conclusions and Future Work

The results prove that GPU computing is very competitive to the traditional approach to high performance computing. Where a single GPU delivers the performance of a whole cluster of HPC-servers. Even for complicated algorithms and data structures as used in the PCG-AMG solver the graphics hardware and programming tools are now mature enough for a successful implementation. Although all results so far have been achieved with single precision arithmetics, double precision hardware will be available soon. With full double precision support and several GB of on–board memory, it can be expected that GPU computing will play a significant role in future HPC applications.

Future work on the PCG-AMG algorithm [2] will be focused on supporting parallel computers with multiple GPU boards. Thus enabling the solution of large scale problems on GPU clusters.

## References

[1] W. L. Briggs, V. E. Henson, and S. McCormick. *A Multigrid Tutorial*. SIAM, second edition, 2000.

[2] G. Haase, M. Kuhn, and S. Reitzinger. *Parallel AMG on distributed memory computers*. SIAM J. Sci. Comput., **24**(2):410–427, 2002.

[3] G. Plank, M. Liebmann, R. Weber dos Santos, E. Vigmond, and G. Haase. *Algebraic multigrid preconditioner for the cardiac bidomain model*. IEEE Transactions on Biomedical Engineering, **54**(4):585–596, 2007.

[4] J. W. Ruge and K. Stüben. *Algebraic multigrid (AMG)*. In S. McCormick, editor, *Multigrid Methods*, volume 5 of Frontiers in Applied Mathematics, pages 73–130. SIAM, Philadelphia, 1986.

[5] S. Sengupta, M. Harris, Y. Zhang, and J. D. Owens. *Scan primitives for GPU computing*. In Graphics Hardware 2007, pages 97–106. ACM, Aug. 2007.

## Manifold Mapping for Two-Level Optimization

Peter W. Hemker, D. Echeverría

Studying the space-mapping iteration technique by Bandler et al. [IEEE Trans. Microwave Theory Tech. 42 (1994) pp. 2536–2544] for the efficient solution of optimization problems, we observe the difference between the solution of the optimization problem and the computed space-mapping solution. We repair this discrepancy by exploiting the correspondence between space-mapping and defect-correction iteration and we construct the manifold-mapping algorithm, which is as efficient as space-mapping but converges to the true solution.

To increase the robustness of the algorithm we introduce a regularization technique based on the generalized singular value decomposition of the linearized fine and coarse manifold representations. As an example of the effect of this technique we show the results for an engineering problem from practice.

Details about the algorithm are found in P.W. Hemker and D. Echeverría, *A trust-region strategy for manifold-mapping optimization*, Journal of Computational Physics 224 (2007) pp. 464-475.

## Low Frequency Stable Maxwell Formulations

Ralf Hiptmair
(joint work with F. Krämer and J. Ostrowski)

**Introduction.** We aim to devise a variational formulation of the full linear Maxwell's equations in frequency domain (angular frequency $\omega > 0$) that remains stable when passing to the stationary limit. We consider the case, where field computation is confined to an artificially bounded domain $\Omega \subset \mathbb{R}^3$ of simple topolgy, see Fig. 1 for a typical geometric situation. Inside $\Omega$ there is an Ohmic conductor occupying the region $\Omega_c$.

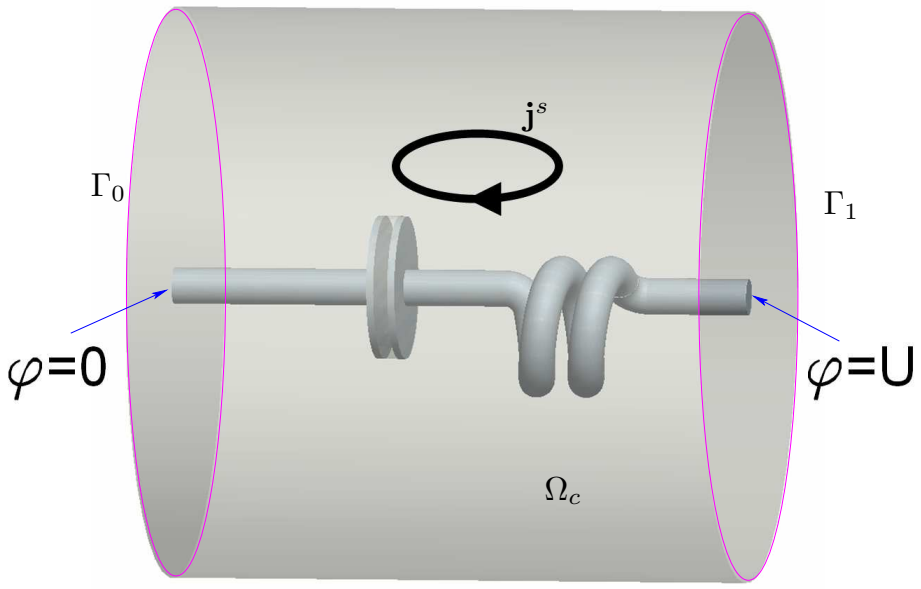


Figure 1. Typical geometry requiring full Maxwell modelling.

Voltage boundary conditions are imposed at $\Gamma_0$ and $\Gamma_1$, whereas ideal coils and space charges may be prescribed inside $\Omega$. In particular, $\mathbf{j}^s = \mathbf{j}_0^s + i\omega\mathbf{j}_1^s$. This provides a setting in which both *inductive and capacitive effects matter*. This rules out using the simpler eddy current model.

We use the Coulomb gauged $\mathbf{a}$-$\varphi$-formulation of Maxwell's equations supplemented with Ohm's law $\mathbf{j} = \sigma\mathbf{e} + \mathbf{j}_0^s$ inside $\Omega_c$. Its variational form relies on the Sobolev spaces

$$V := \{\mathbf{v} \in \boldsymbol{H}(\mathbf{curl}, \Omega) \colon \mathbf{curl}_\Gamma \mathbf{v}_t = 0 \text{ on } \partial\Omega, \int_\tau \mathbf{v} \cdot \vec{\mathrm{d}}s = 0\},$$

$$H(U) := \{\psi \in H^1(\Omega) \colon \psi_{|\Gamma_0} = 0, \psi_{|\Gamma_1} = U\} ,$$

and reads: seek $\mathbf{a} \in V$, $\varphi \in H(U)$ such that

$$
\begin{aligned}
&(\mu^{-1}\,\mathbf{curl}\,\mathbf{a}, \mathbf{curl}\,\mathbf{a}') - \omega^2(\epsilon\mathbf{a}, \mathbf{a}') + i\omega(\sigma\mathbf{a}, \mathbf{a}') \\
&\quad +((i\omega\epsilon + \sigma)\,\mathrm{grad}\,\varphi, \mathbf{a}') = (\mathbf{j}^s, \mathbf{a}')\,, \\
&\qquad (\epsilon\mathbf{a}, \mathrm{grad}\,\varphi') = 0\,,
\end{aligned}
\tag{1}
$$

for all $\mathbf{a}' \in V$, $\varphi' \in H(0)$ ($(\cdot,\cdot) \mathrel{\hat{=}} L^2$ inner product).

**Low-frequency instability.** It is well known that Gauss' law $\mathrm{div}(\epsilon\mathbf{e}) = \rho$ is contained in (1) for any $\omega > 0$, but becomes an independent equation in $\Omega_e := \Omega \setminus \overline{\Omega}_c$ in the stationary limit $\omega = 0$. This decoupling manifests itself as a loss of control of the scalar potential $\varphi$ in $\Omega_e$ in (1) as $\omega \to 0$. In mathematical terms, the norm of the solution operator for (1) will blow up as $\omega \to 0$; (1) lacks uniform stability as $\omega \to 0$, since the recovery of $\varphi$ becomes ill-posed. Eventually, even round-off errors will severely pollute any approximate solution for $\varphi$.

**Generating system approach.** Ill-conditioned discrete variational problems can often be stabilized by augmenting the underlying basis with additional vectors in the span of the basis, thus obtaining a *generating system*. Using it to "discretize" the variational problem yields a *singular* matrix.

The key observation is that most iterative solvers can well cope with singular matrices provided that the right hand sides of the linear systems are consistent [1]: crucial is the distribution of *non-zero* eigenvalues, which indicates the stability of the generating system. It is worth noting that the very same augmentation idea accounts for the power of multigrid methods [2, 3] and has been used to enhance ILU-preconditioners in [4]. The idea is also related to recent attempts to use frames for the discretization of operator equations [5, 6].

**Stabilzed variational formulation.** Our generating systems approach boils down to using *non-direct* decompositions of trial and test spaces. For (1) we may use the non-direct splitting

$$
\begin{aligned}
&H(U) = H(U)' + H^1_e(\Omega)\,, \\
&H^1_e(\Omega) := \left\{ \begin{array}{l} v \in H^1(\Omega):\ v \equiv \text{const on all connected components of } \Omega_c, \\ v_{|\Gamma_0} = 0,\ v_{|\Gamma_1} = 0\,. \end{array} \right\}.
\end{aligned}
$$

Accordingly, in (1) we replace $\varphi$ with the sum $\varphi = \tilde{\varphi} + \psi$, $\tilde{\varphi} \in H(U)$, $\psi \in H^1_e(\Omega)$. The introduction of an extra unknown has to be balanced by an extra equation, which we obtain by testing the first equation of (1) with $\psi' \in H^1_e(\Omega)$.

Note that $\mathrm{grad}\,\psi' \equiv 0$ inside $\Omega_C$: the extra equation is redundant for any $\omega > 0$, but after dividing by $i\omega$ it represents Gauss' law in the non-conducting domain. This is exactly the information that is missing (1) in the stationary limit.

Eventually, we arrive at the following variational problem: seek $\mathbf{a} \in V$, $\tilde{\varphi} \in H(U)$, $\psi \in H^1_e(\Omega)$ such that for all $\mathbf{a} \in V$, $\tilde{\varphi}' \in H(0)$, $\psi' \in H^1_e(\Omega)$

$$
\begin{aligned}
&(\mu^{-1}\,\mathbf{curl}\,\mathbf{a}, \mathbf{curl}\,\mathbf{a}') - \omega^2(\epsilon\mathbf{a}, \mathbf{a}') + i\omega(\sigma\mathbf{a}, \mathbf{a}') + \\
&\quad ((i\omega\epsilon + \sigma)\,\mathrm{grad}\,\tilde{\varphi}, \mathbf{a}') + i\omega(\epsilon\,\mathrm{grad}\,\psi, \mathbf{a}') = \quad (\mathbf{j}^s, \mathbf{a}')\,, \\
&\qquad\qquad (\epsilon\mathbf{a}, \mathrm{grad}\,\tilde{\varphi}') \quad = \quad 0\,, \\
&(\epsilon\,\mathrm{grad}\,\tilde{\varphi}, \mathrm{grad}\,\psi') + (\epsilon\,\mathrm{grad}\,\psi, \mathrm{grad}\,\psi') \quad = (\mathrm{div}\,\mathbf{j}^s_1, \psi')\,.
\end{aligned}
\tag{2}
$$

If $(\mathbf{a}, \varphi)$ solves (1), then the same functions together with $\psi = 0$ will supply a solution of (2). Fittingly, in (2) the second equation arises from combining the first and the third. Both observations remain valid also after discretization by means of conforming finite elements, that is, in the case of edge element approximation for $\mathbf{a}$ and continuous piecewise linear element used for $\tilde{\varphi}$ and $\psi$. Consequently, the linear systems of equations arising from (2) will be square but *singular*, which is natural for the generating systems approach.

**Stationary limit.** Setting $\omega = 0$ (stationary limit) in (2) perfectly decouples the system into the familiar and stable variational problems of stationary electromagnetism:

First, we recover the stationary currents boundary value problem inside the conductor and the electrostatic potential equation in $\Omega_e$ through testing the first equation with gradients, and using the second: find $\varphi \in H(U)$ with

$$(\sigma \operatorname{grad} \varphi, \operatorname{grad} \varphi')_{\Omega_c} = 0 \quad \forall \varphi' \in H(0) \,. \tag{3}$$

$$(\epsilon \operatorname{grad} \varphi, \operatorname{grad} \psi') = (\operatorname{div} \mathbf{j}_1^s, \psi') \quad \forall \psi' \in H_e^1(\Omega) \,. \tag{4}$$

Charge balance is hidden in the second variational equation, because integration by parts reveals $\int_{\partial\Omega_c} \epsilon \operatorname{grad} \varphi \cdot \mathbf{n} \, \mathrm{d}S = \int_{\partial\Omega_c} \mathbf{j}_1^s \cdot \mathbf{n} \, \mathrm{d}S$. The source term $\mathbf{j}_1^s$ enables us to fix the total charge of connected components of the conductor, which is another freedom in the stationary limit.

Second, the equations of magnetostatics emerge from the first and second equation of (2): with $\varphi$ from (3), (4), seek $\mathbf{a} \in V$ such that for all $\mathbf{a}' \in V$, $\varphi' \in H(0)$

$$(\mu^{-1} \mathbf{curl}\, \mathbf{a}, \mathbf{curl}\, \mathbf{a}') = (\mathbf{j}^s, \mathbf{a}') - (\sigma \operatorname{grad} \varphi, \mathbf{a}') \,, \; (\epsilon \mathbf{a}, \operatorname{grad} \varphi') = 0 \,.$$

The bottom line is that the limit equations are perfectly well-posed, which bodes well for the behavior of iterative solvers when applied to a discretized version of (2): we can expect *robustness* with respect to small values of $\omega$, which is confirmed by first numerical experiments reported in [7].

## References


[1] M. Hochbruck and C. Lubich, "Error analysis of Krylov methods in a nutshell," *SIAM J. Sci. Comput.*, vol. 19, pp. 695–701, 1998.

[2] M. Griebel, "Multilevel algorithms considered as iterative methods on semidefinite systems," *SIAM J. Sci. Stat. Comp.*, vol. 15, pp. 547–565, 1994.

[3] B. Weiss and O. Biro, "Multigrid for time-harmonic 3-d eddy-current analysis with edge elements," *IEEE Trans. Magnetics*, vol. 41, no. 5, pp. 1712–1715, 2005.

[4] H. Igarashi and T. Honma, "On convergence of iccg applied to finite-element equation for quasi-static fields," *IEEE Trans. Magnetics*, vol. 38, no. 2, pp. 565–568, 2002.

[5] S. Dahlke, M. Fornasier, and T. Raasch, "Adaptive frame methods for elliptic operator equations," *Adv. Comp. Math.*, vol. 27, pp. 27–63, 2007.

[6] R. Stevenson, "Adaptive solution of operator equations using wavelet frames," *SIAM J. Numer. Anal.*, vol. 41, no. 3, pp. 1074–1100, 2003.

[7] R. Hiptmair, F. Krämer, and J. Ostrowski, "Robust Maxwell formulations," *IEEE Trans. Magnetics*, vol. 44, no. 6, pp. 682–685, 2008.

## Analysis and Adaptive treatment of a geometric PDE in Mathematical Physics.

Michael Holst

The Einstein constraint equations have been studied intensively for half a century; our foces in this lecture is on a thirty-year old open question involving existence of solutions to the constraint equations on space-like hyper-surfaces with arbitrarily prescribed mean curvature, and on the develpment of a provably convergent adaptive numerical method. All known existence results have involved assuming either constant (CMC) or nearly-constant (near-CMC) mean extrinsic curvature. After giving a survey oh known CMC and near-CMC conditions through 2007, we outline a new topological fixed-point framework that is fundamentally free of both CMC and near-CMC conditions, resting on the construction of "global barriers" for the Hamiltonian constraint. We then present such a barrier construction for the case of closed manifolds with positive Yamabe metrics, giving the first known existence results for arbitrarily prescribed mean extrinsic curvature. Our results are devloped in the setting of a "weak" background metric which requires building up a set of premilinary results on Sobolev classes and elliptic operators on manifolds with weak metrics. This allows us to recover the recent "rough" CMC existence results of Choquet-Bruhat (2004) and of Maxwell (2004, 2006) as two distinct limiting cases of our non-CMC results. Our results also extend to other case such as compact manifolds with boundary. We then describe an AFEM algorithm based on a standard SOLVE-ESTIMATE-MARK-REFINE procedure, and establish that it is a constraction when applied to the Hamiltonian constraint. The proof uses a nonlinear extension of the 2007 article of Cason et al., based on a nonlinear indicator reduction lemma and a nonlinar quasi-orthogonality result.

## Adaptive Multilevel Primal-Dual Interior-Point Methods in PDE Constrained Optimization

Ronald H.W. Hoppe

(joint work with Harbir Antil, Christopher Linsenmann)

We are concerned with structural optimization problems where the state variables are supposed to satisfy a PDE or a system of PDEs and the design variables are subject to inequality constraints. A typical shape optimization problem associated with a time-independent PDE or a system thereof as the underlying state equation amounts to the minimization of a shape functional $J$ over bounded domains $\Omega$ in Euclidean space $\mathbb{R}^d$. The state function $u$ is assumed to satisfy a boundary value problem as described by means of a partial differential operator $L$, and there may be further equality and/or inequality constraints on the domain.

$$\inf_{\Omega} J(u,\Omega) \quad , \quad J(u,\Omega) := \int_{\Omega} j(x,u(x))\, dx, \tag{1a}$$

$$\text{subject to } Lu = f \quad \text{in } \Omega \quad , \quad u = g \quad \text{on } \Gamma \quad , \quad h(\Omega) \geq 0. \tag{1b}$$

The inherent difficulty that the minimization is over a certain class of domains instead of a set of functions in an appropriate function space can be circumvented based on a parametrization of the domain by a finite number of design variables. In particular, the design variables are chosen as the Bézier control points $\alpha \in \mathbb{R}^m, m \in \mathbb{N}$, of a composite Bézier curve representation of the boundary $\Gamma$. The inequality constraints are expressed by means of the design variables as well. For the numerical solution of (1a)-(1b) we use a finite element discretization of (1a)-(1b) with respect to a simplicial triangulation $\mathcal{T}_h(\Omega(\alpha))$ of the computational domain $\Omega(\alpha)$. This leads to a finite dimensional optimization problem

$$\inf_{u_h,\alpha} J_h(u_h,\alpha), \tag{2a}$$

$$\text{subject to } L_h u_h \;=\; b_h \;,\; h(\alpha) \;\geq\; 0, \tag{2b}$$

where $u_h \in \mathbb{R}^n$ is the finite element approximation of the state $u$, $J_h(u_h,\alpha)$ the discretized objective functional and $L_h u_h = b_h$ the algebraic system arising from the finite element discretization of the PDE.
The inequality constraints in (1b) are coupled by logarithmic barrier functions with a barrier parameter $\beta = 1/\mu > 0$, $\mu \to \infty$, and the equality constraint by a Lagrange multiplier $\lambda_h \in \mathbb{R}^n$. This leads to the saddle point problem

$$\inf_{u_h,\alpha} \sup_{\lambda_h} \mathcal{L}_h^{(\mu)}(u_h,\lambda_h,\alpha) \;. \tag{3}$$

Here, $\mathcal{L}_h^{(\mu)}$ is the Lagrangian

$$\mathcal{L}_h^{(\mu)}(u_h,\lambda_h,\alpha) \;=\; B^{(\mu)}(u_h,\alpha) \;+\; \langle \lambda_h, L_h u_h - b_h \rangle \tag{4}$$

with $B^{(\mu)}(u_h,\alpha)$ denoting the so-called barrier function

$$B^{(\mu)}(u_h,\alpha) \;:=\; J_h(u_h,\alpha) \;-\; \frac{1}{\mu}\ln(h(\alpha)) \;. \tag{5}$$

and $\langle \cdot,\cdot \rangle$ the Euclidean inner product on $\mathbb{R}^n$. The barrier path $\mu \longmapsto x_h(\mu) := (u_h(\mu),\lambda_h(\mu),\alpha(\mu))^T$ is given as the solution of the nonlinear system

$$F(x_h(\mu),\mu) \;=\; \begin{pmatrix} \partial_{u_h}\mathcal{L}_h^{(\mu)}(u_h,\lambda_h,\alpha) \\ \partial_{\lambda_h}\mathcal{L}^{(\mu)}(u_h,\lambda_h,\alpha) \\ \partial_{\alpha}\mathcal{L}^{(\mu)}(u_h,\lambda_h,\alpha) \end{pmatrix} \;=\; 0 \;, \tag{6}$$

where the subindices refer to the derivatives of the Lagrangian with respect to the primal, the dual, and the design variables.
We solve (5) by an adaptive continuation method based on the affine invariant convergence theory of Newton-type methods. The adaptive continuation method is a predictor-corrector method with an adaptively determined continuation step size in the predictor and Newton's method as a corrector. It relies on the affine invariant convergence theory of Newton and Newton-type methods and ensures that the iterates stay within a neighborhood (contraction tube) of the barrier path so that convergence to a local minimum of the original minimization problem can be achieved. Given some approximation for $x_h(\mu) = (u_h(\mu),\lambda_h(\mu),\alpha(\mu))^T$ at $\mu_k$, the predictor step relies on tangent continuation along the trajectory of the

Davidenko equation $F_{x_h}(x_h(\mu),\mu)\ x_h'(\mu) = -F_\mu(x_h(\mu),\mu)$ and amounts to the implementation of an explicit Euler step. As a corrector, we use Newton's method applied to $F(x_h(\mu_{k+1}),\mu_{k+1}) = 0$ with the prediction as the start vector. A monotonicity test based on a simplified Newton correction checks contractivity. If it fails, the continuation step has to be repeated with a reduced steplength (see [1]).

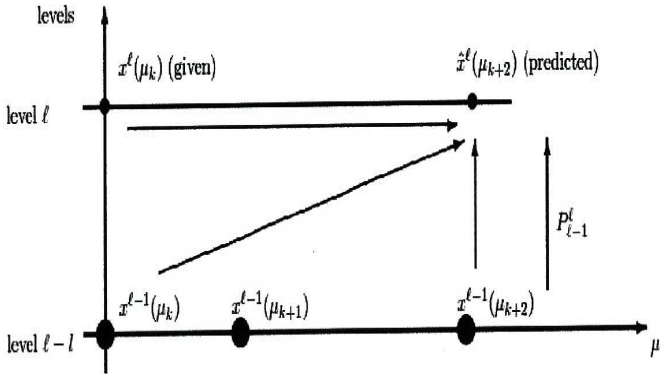


FIGURE 1. Two-level predictor-corrector scheme

The predictor-corrector scheme is realized within a multilevel framework with respect to a hierarchy of discretizations. In case of a two-level scheme with the levels $\ell-1$ and $\ell$ (cf. Fig. 1), the prediction is done by nested iteration in such a way that a certain number of adaptive continuation steps are performed on the coarser level $\ell-1$ before a predicted value is computed on the finer level $\ell$. The corrector is a Newton multigrid method incorporating a two-level PDE solver featuring appropriate smoothers. The iterates are checked for acceptance by the level $\ell$ monotonicity test. In the general case of more than 2 levels, the multilevel predictor-corrector continuation method consists of a recursive application of the two-level scheme (see [2] for details).

As an application, we consider the optimal design of capillary barriers in microfluidic biochips that are used in pharmaceutical, medical and forensic applications for high throughput screening, genotyping and sequencing by hybridization in genomics, protein profiling in proteomics, and cytometry in cell analysis (see [3]). Recent nanotechnological devices are biochips with integrated fluidics on top of the chip consisting of a lithographically produced network of channels and reservoirs. Between the channels and the reservoirs are pressure driven capillary barriers (cf. Fig. 2 (left)) which have to be designed in such a way that a precise filling of the reservoirs is guaranteed.

The objective functional is of tracking type, whereas the state equations are given by a Stokes system with Signorini type boundary conditions at the outflow boundary for modeling the barrier. Fig. 2 (right) shows a visualization of the velocity field in the flow mode for the optimized geometry of the barrier.

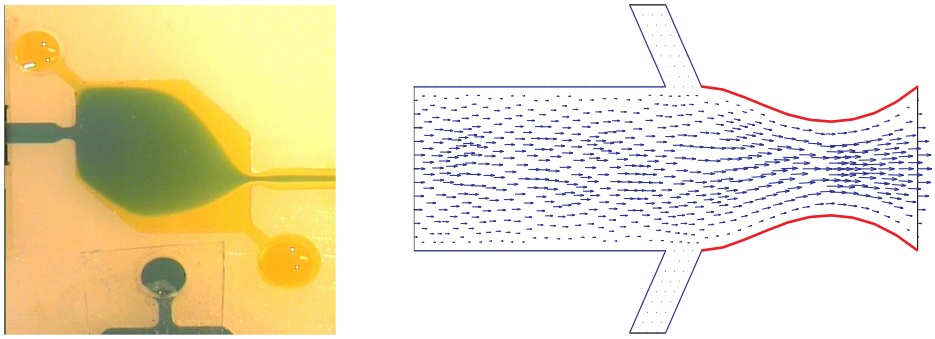

FIGURE 2. Capillary barrier and reservoir (left) and velocity field for an optimized design of the barrier (right)

## REFERENCES

[1] H. Antil, R.H.W. Hoppe, and C. Linsenmann; Path-following primal-dual interior-point methods for shape optimization of stationary flow problems. Journal of Numerical Mathematics **11**, 81–100, 2007

[2] H. Antil, R.H.W. Hoppe, and C. Linsenmann; Adaptive multilevel interior-point methods in PDE constrained. submitted to Proc. 18th Int. Conf. on Domain Decompostion Methods and Applications, Lecture Notes in Science and Engrg., Springer, Berlin-Heidelberg-New York, 2008

[3] A. Gantner, R.H.W. Hoppe, D. Köster, K.G. Siebert, and A. Wixforth; Numerical simulation of piezoelectrically agitated surface acoustic waves on microfluidic biochips. Comput. Visual. Sci. **10**, 145-161, 2007

## Tensor Approximation of Multidimensional Operators with Applications

BORIS N. KHOROMSKIJ

We describe a novel tensor approximation method for discretised multidimensional functions and operators in $\mathbb{R}^d$, based on the idea of multigrid acceleration presented in [4]. The approach stands on successive reiterations of the orthogonal Tucker tensor approximation on a sequence of nested refined grids. On the one hand, it provides a good initial guess for the nonlinear iterations to find the approximating subspaces on finer grids, on the other hand, it allows to transfer from the coarse-to-fine grids the important data structure information on location of the so-called most important fibers in directional unfolding matrices. The method indicates linear complexity with respect to the size of data representing the input tensor.

The method is tested by 3D electronic structure calculations. For the multigrid accelerated low Tucker-rank approximation of the all electron densities having strong nuclear cusps, we obtain high resolution of their 3D convolution product with the Newton potential. The accuracy of order $10^{-6}$ in max-norm is achieved on large $n \times n \times n$ grids up to $n = 1.6 \cdot 10^4$, with the time scale in several minutes.

Some related topics of tensor methods can be found in [1] - [3].

References

[1] H.-J. Flad, B. Khoromskij, D. Savostianov, and E. Tyrtyshnikov: *Verification of the cross 3d algorithm on quantum chemistry data.* Rus. J. Numer. Anal. and Math. Modelling, vol. 4, 2008 (1-16), (to appear).

[2] W. Hackbusch and B.N. Khoromskij: *Low-rank Kronecker product approximation to multi-dimensional nonlocal operators. Part I. Separable approximation of multi-variate functions.* Computing **76** (2006), 177-202.

[3] B. N. Khoromskij, *Multi-linear approximation of higher-dimensional convolution in linear cost.* Preprint MPI MIS 36, 2008, Leipzig (submitted).

[4] B. N. Khoromskij and V. Khoromskaia, *Multigrid accelerated tensor approximation of function related multi-dimensional arrays.* Preprint MPI MIS 40, 2008, Leipzig (submitted).

## Preconditioned nullspace method for the Oseen problem

Sabine Le Borne

The Oseen problem, which arises in the simulation of the time-dependent Navier-Stokes equations for incompressible fluid flow, leads to indefinite, non-symmetric and possibly ill-conditioned linear systems of equations. This talk presents a method to obtain a reduced linear system from the original system which is then solved by the preconditioned GMRES method. The system reduction is obtained through an efficient implicit representation of a basis of discretely divergence free functions, also known as the *nullspace method*. We will analyse the spectrum of the preconditioned reduced system, and present numerical tests to illustrate the performance of this method which shows only mild dependence on the mesh size and viscosity dominance.

As a model problem, we consider the Oseen equations: Let $\Omega \subset \mathbb{R}^d$, $(d \in \{2,3\})$, denote a bounded, connected domain with a piecewise smooth boundary $\Gamma$. Given a force field $f : \Omega \to \mathbb{R}^d$, boundary data $g : \Gamma \to \mathbb{R}^d$, the kinematic viscosity coefficient $\epsilon$, and a given, divergence-free coefficient $b : \Omega \to \mathbb{R}^d$, the problem is to find the velocity field $u : \Omega \to \mathbb{R}^d$ and the pressure $p : \Omega \to \mathbb{R}$ such that the Oseen equations

$$\begin{aligned} -\epsilon\Delta u + (b\cdot\nabla)u + \nabla p &= f \quad \text{in } \Omega, \\ -\mathrm{div} u &= 0 \quad \text{in } \Omega, \\ Cu &= g \quad \text{on } \Gamma, \end{aligned}$$

are satisfied. Here, $C$ denotes some type of boundary operator. A *stable* mixed finite element discretization of the Oseen equations leads to a system of equations of the form

$$\begin{pmatrix} A & B \\ B^T & 0 \end{pmatrix} \begin{pmatrix} x \\ y \end{pmatrix} = \begin{pmatrix} f \\ g \end{pmatrix} \tag{1}$$

where $A \in \mathbb{R}^{n\times n}$ and $B \in \mathbb{R}^{n\times m}$ with $m < n$.

In order to employ the nullspace method to solve the linear system (1), we will make the following assumptions:

- $B \in \mathbb{R}^{n\times m}$ has full rank $m$;
- $\ker(A + A^T) \cap \ker(B^T) = \{0\}$ (which guarantees that the saddle point matrix in (1) is invertible);
- A particular solution $\hat{x}$ of $B^T x = g$ is available;
- A null space basis $Z \in \mathbb{R}^{n\times(n-m)}$ of $B^T$ is available, i.e.,

$$B^T Z = 0 \quad \text{and} \quad \operatorname{rank}(Z) = n - m.$$

The required particular solution $\hat{x}$ may be computed through $\hat{x} = B(B^T B)^{-1} g$. The solution set of $B^T x = g$ is described by $x = Zv + \hat{x}$ as $v$ ranges in $\mathbb{R}^{n-m}$. Substituting $x = Zv + \hat{x}$ in $Ax + By = f$, we obtain $A(Zv + \hat{x}) + By = f$. Premultiplying by the full-rank matrix $Z^T$ yields $Z^T A(Zv + \hat{x}) + Z^T By = Z^T f$, and using $B^T Z = 0$ as well as rearranging the equation yields the reduced, non-singular problem

$$Z^T AZv = Z^T(f - A\hat{x}).$$

Once the solution $v_*$ of the reduced problem has been computed, we set $x_* = Zv_* + \hat{x}$. Finally, the solution $y_*$ can be found by solving $B^T By = B^T(f - Ax_*)$ for $y$, a reduced system of order $m$ with a sparse, symmetric positive definite coefficient matrix $B^T B$.

The construction and representation of an orthogonal nullbasis of the discrete divergence operator $B^T$ is based on the following two observations:

- The last $n - m$ columns of the orthogonal factor $Q = [Y\ Z] \in \mathbb{R}^{n\times n}$, with $Z \in \mathbb{R}^{n\times(n-m)}$, in a full QR factorization $B = QR$, form an orthogonal null basis of $B^T$.
- The orthogonal factor $Q$ in a full QR factorization $B = QR$ of a discrete (finite element/finite difference) gradient $B$ has an efficient block representation which is presented in Theorem 1 [1].

**Theorem 1.** *Let* $B = \begin{pmatrix} B_1 \\ B_2 \end{pmatrix} \in \mathbb{R}^{n\times m}$ *with* $B_1 \in \mathbb{R}^{m\times m}, B_2 \in \mathbb{R}^{(n-m)\times m}$ *and* $\operatorname{rank}(B) = m$. *Let* $R \in \mathbb{R}^{m\times m}$ *denote the upper triangular Cholesky factor of* $B^T B$. *Under the additional assumption that the LU factorization of* $B_1 - R$ *exists, we denote these LU factors by* $V, W$ *(i.e.,* $B_1 - R = VW$*). Then an orthogonal null basis of* $B^T$ *is represented by*

$$Z = \begin{pmatrix} 0 \\ I_2 \end{pmatrix} + \begin{pmatrix} B_1 R^{-1} - I_1 \\ B_2 R^{-1} \end{pmatrix} V^{-T} W^{-T} B_2^T. \tag{2}$$

Whereas the representation (2) is valid for arbitrary rectangular matrices $B = \begin{pmatrix} B_1 \\ B_2 \end{pmatrix} \in \mathbb{R}^{n\times m}$, it becomes particularly efficient when applied to finite element matrices $B$ after certain row and column reorderings, i.e., when applied to $\tilde{B} := P_r B P_c$ with permutation matrices $P_r$, $P_c$. In particular, it is proposed to choose $P_c$ as a nested dissection ordering of the column index set to facilitate the Cholesky factorization of $\tilde{B}^T \tilde{B}$. If an exact Cholesky factorization is too expensive, it may be replaced by an approximation (e.g., incomplete Cholesky or hierarchical matrix Cholesky factorization). The row permutation $P_r$, on the other side, has no impact

on the Cholesky factorization and is chosen to facilitate the LU factorization of $\tilde{B}_1 - R$. In particular, with $P_c$ given already, $P_r$ is chosen so that $\tilde{B}_1$ becomes "almost" upper triangular, i.e., has as few as possible entries in its lower triangular part. For further details on this implicit null basis representation and suitable orderings we refer to [1].

In order to solve the reduced system $Z^T AZv = Z^T(f - A\hat{x})$, we use a preconditioned GMRES method with preconditioner $Z^T\tilde{A}^{-1}Z$ where $\tilde{A}^{-1}$ is an approximation of $A^{-1}$. In our subsequent numerical results, we use an $\mathcal{H}$-LU factorization of $A$ to obtain $\tilde{A}^{-1}$. In the case of $\tilde{A}^{-1} = A^{-1}$, one obtains the following result on the eigenvalues of the preconditioned matrix.

**Theorem 2.** *Let $Q = [Y\ Z]$, $Y \in \mathbb{R}^{n\times m}$ be the orthogonal factor in the QR-factorization of $B$. The spectrum of $Z^T A^{-1} ZZ^T AZ$ satisfies*

$$\lambda(Z^T A^{-1} ZZ^T AZ) \subset \{1\} \cup \{1 - \lambda_i(Y^T A^{-1} ZZ^T AY) \mid i = 1, \ldots, m\}.$$

*In particular, there are at most $m$ eigenvalues not equal to one.*

In Table 3, we show numerical results for the Oseen problem in two spatial dimensions. We use $\mathcal{H}$-arithmetic with adaptive accuracy $\delta = 10^{-8}$ to compute an $\mathcal{H}$-LU factorization of $A$ which is used as $\hat{A}^{-1}$ and an $\mathcal{H}$-Cholesky factorization of $B^T B$ to obtain an approximate null basis $\hat{Z}$ (see, e.g., [2] for further details on $\mathcal{H}$-matrices). We record the number of GMRES steps as well as the required time (in seconds) to reduce the residual by a factor of $10^{-6}$. At this point, we only compute solutions for the velocity but not the pressure. (Once the velocity is available, the pressure can be computed through a triangular solve with $R$ since $Y^T B = R$). All numerical tests have been performed on a Dell 690n workstation (2.33GHz, 32GB memory) using the standard $\mathcal{H}$-matrix library HLib (cf. `http://www.hlib.org`).

In Table 3, we show results for varying convection dominance (through the choice of $\epsilon$ in the Oseen problem) and convection directions $b_{xline}(x, y) = (1, 0)^T$, $b_{circ}(x, y) = (-y,\ x)^T$, as well as $b_{recirc}(x, y) = \left(-(x^2 - 1)y,\ (y^2 - 1)x\right)^T$. The results show some dependence on the convection direction, but only a very moderate dependence on the convection dominance and the problem size.

Future work includes the application of the proposed preconditioned nullspace method to problems of three spatial dimensions as well as sequences of saddle point problems in time dependent problems.

## References

[1] S. Le Borne, *Block computation and representation of a sparse nullspace basis of a rectangular matrix*, Lin. Alg. Appl. **428** (2008), 2455–2467.

[2] S. Börm, L. Grasedyck and W. Hackbusch *Hierarchical Matrices*, Lecture Notes No. 21, Max-Planck-Institute for Mathematics in the Sciences, Leipzig, Germany, available online at www.mis.mpg.de/preprints/ln/, revised version June 2006,

TABLE 3. Preconditioned nullspace method: GMRES steps (and time in seconds) for fixed $\mathcal{H}$-accuracy $\delta = 10^{-8}$

| $n-m$ | | 70,398 | 137,758 | 280,798 | 561,753 | 1,121,598 |
|---|---|---|---|---|---|---|
| $b = b_{xline}$ | $\epsilon = 0.1$ | 17 (3.0) | 18 (6.5) | 20 (15) | 23 (37) | 24 (75) |
| | $\epsilon = 10^{-2}$ | 11 (2.0) | 13 (4.8) | 15 (11) | 18 (29) | 21 (65) |
| | $\epsilon = 10^{-3}$ | 9 (1.6) | 9 (3.3) | 8 (6.2) | 8 (13) | 8 (26) |
| $b = b_{circ}$ | $\epsilon = 0.1$ | 21 (3.7) | 24 (8.6) | 26 (19) | 30 (48) | 33 (103) |
| | $\epsilon = 10^{-2}$ | 21 (3.6) | 24 (8.6) | 29 (22) | 34 (54) | 40 (126) |
| | $\epsilon = 10^{-3}$ | 28 (4.6) | 30 (10.4) | 31 (22) | 34 (53) | 37 (113) |
| $b = b_{recirc}$ | $\epsilon = 0.1$ | 19 (3.3) | 22 (8.0) | 25 (19) | 28 (45) | 31 (96) |
| | $\epsilon = 10^{-2}$ | 20 (3.4) | 23 (8.2) | 27 (20) | 32 (51) | 36 (112) |
| | $\epsilon = 10^{-3}$ | 37 (6.0) | 38 (13) | 40 (29) | 42 (65) | 46 (140) |

## On the Use of Linear Programming to Compute Sparse Approximate Solutions of PDEs

VOLKER MEHRMANN

(joint work with Sadegh Jokar, Marc Pfetsch, Harry Yserentant)

The sparse representation of functions via a linear combination of a small number of basic functions has recently received a lot of attention in several mathematical fields such as approximation theory [11, 23, 25, 26] as well as signal and image processing [3–9, 12–18]. In terms of representations of functions, we can describe the problem as follows. Consider a linearly dependent set of $n$ functions $\phi_i$, $i = 1, 2, \ldots, n$, (*a dictionary* [10]) and a function $f$ represented as

$$f = \sum_{i=1}^{n} x_i \, \phi_i.$$

Since the set of functions is not linearly independent, this representation is not unique and we may want to determine the sparsest representation, i.e., a representation with a maximal number of vanishing coefficients among $x_1, \ldots, x_n$.

In the setting of numerical linear algebra, this problem can be formulated as follows. Consider a linear system

$$\Phi x = b, \tag{1}$$

with $\Phi \in \mathbb{R}^{m,n}$, where $m \leq n$ and $b \in \mathbb{R}^m$. The columns of the matrix $\Phi$ and the right hand side $b$ represent the functions $\phi_i$ and the function $f$, respectively, with respect to some basis of the relevant function space. The problem is then to find the sparsest possible solution $x$, i.e., $x$ has as many zero components as possible. This optimization problem is in general NP-hard [19, 24]. Starting from the work of [9], however, a still growing number of articles have developed sufficient conditions that guarantee that an (approximate) sparse solution $\hat{x}$ to (1) can be

obtained by solving the linear program

$$\min \|x\|_1, \ s.t. \ \Phi x = b,$$

which can be done in polynomial time [21, 22].

In the literature, the development has mostly focused on the construction of appropriate coding matrices $\Phi$ that allow for the sparse representation of a large class of functions (signals or images). Furthermore, properties of the columns of the matrix (or the dictionary) have been investigated, which guarantee that the computation of the sparse solution can be done efficiently via a linear programming approach, see, for instance, [8, 20]. Often the term *compressed sensing* is used for this approach.

We consider a related but different problem. We are interested in the numerical solution of partial differential equations

$$Lu = f,$$

with a differential operator $L$, to be solved in a domain $\Omega \subset \mathbb{R}^d$ with smooth boundary $\Gamma$ and appropriate boundary conditions given on $\Gamma$.

Considering a classical Galerkin or Petrov-Galerkin finite element approach, see e.g. [2], one seeks a solution $u$ in some function space $\mathbb{U}$ (which is spanned by $\phi_1, \ldots, \phi_n$), represented as

$$u = \sum_{i=1}^{n} u_i \, \phi_i. \tag{2}$$

Again we are interested in sparse representations with a maximal number of vanishing coefficients $u_i$. In contrast to the cases discussed before, here we would like to construct the space $\mathbb{U}$ and the basis functions $\phi_i$ in the finite element discretization in such a way that first of all a sparse representation of the solution to (2) exists and second that it can be determined efficiently. Furthermore, it would be ideal if the functions $\phi_i$ could be constructed in a multilevel or adaptive way.

The usual approach to achieve this goal is to use local a posteriori error estimation to determine where a refinement, i.e., the addition of further basis functions is necessary. For example, in the dual weighted residual approach [1] this is done by solving an optimization problem for the error.

Here, we examine the possibility to use similar approaches as those used in compressed sensing, i.e., to use $\ell_1$-minimization and linear programming to perform the adaptive refinement in the finite element method in such a way that the solution is sparsely represented by a linear combination of basis functions. In order to achieve this goal, we propose the following framework.

We determine $u \in \mathbb{U}$ as the solution of the weak formulation

$$(v, Lu - f) = 0 \quad \text{for all} \quad v \in \mathbb{V}.$$

Here, $\mathbb{V}$ is a space of test functions and $(\cdot,\cdot)$ is an appropriate inner product. In the simplest version of a two-level approach, we construct finite dimensional spaces of coarse and fine basis functions $\mathbb{U}_1^n \subset \mathbb{U}_1^N \subset \mathbb{U}$ and corresponding spaces for coarse

and fine test functions $\mathbb{V}_1^n \subset \mathbb{V}_1^N \subset \mathbb{V}$. Then we determine the approximate sparsest solution in $\mathbb{U}_1^N$, such that

$$(v, Lu - f) = 0 \quad \text{for all } v \in \mathbb{V}_N^1 \setminus \mathbb{V}_n^1$$

via the solution of an underdetermined system of the form (1). Based on the sparse solution, we determine new coarse and fine spaces $\mathbb{U}_2^n \subset \mathbb{U}_2^N \subset \mathbb{U}$, $\mathbb{V}_2^n \subset \mathbb{V}_2^N \subset \mathbb{V}$, and iterate this procedure.

This framework combines the ideas developed in compressed sensing with well-known concepts arising in adaptive and multilevel finite element methods. But instead of using local and global error estimates to obtain error indicators by which the grid refinement is controlled, here the solution of the $\ell_1$-minimization is used to control the grid refinement and adaptivity.

However, many issues of this approach have not yet been resolved, in particular, the theoretical analysis of this approach. We see the following potential advantages and disadvantages of this framework. On the positive side, the $\ell_1$-minimization approach allows for an easy automation. On the downside, the analysis of the approach seems to be hard even for classical elliptic problems, and due to the potentially high complexity of the linear programming methods this approach will only be successful if the procedure needs only a few levels and a verysmall sparse representation of the solution exists.

## References


[1] R. Becker and R. Rannacher, *An optimal control approach to a posteriori error estimation in finite element methods*, in Acta Numerica, no. 10, Cambridge University Press, (2001), pp. 1–102.

[2] D. Braess, *Finite Elements: Theory, Fast Solvers and Applications in Solid Mechanics*, Cambridge, Cambridge University Press, 3rd ed., (2007).

[3] E. J. Candés, *Compressive sampling*, in Proc. International Congress of Mathematics, Madrid, Spain, (2006), pp. 1433–1452.

[4] E. J. Candès and J. Romberg, *Quantitative robust uncertainty principles and optimally sparse decompositions*, Found. Comput. Math. **6**, no. 2 (2006), pp. 227–254.

[5] E. J. Candès, J. Romberg, and T. Tao, *Robust uncertainty principles: Exact signal reconstruction from highly incomplete frequency information*, IEEE Trans. Inform. Theory **52**, no. 2 (2006), pp. 489–509.

[6] E. J. Candès, J. Romberg, and T. Tao, *Stable signal recovery from incomplete and inaccurate measurements*, Comm. Pure Appl. Math. **59**, no. 8 (2006), pp. 1207–1223.

[7] E. J. Candès and T. Tao, *Decoding by linear programming*, IEEE Trans. Inform. Theory **51**, no. 12 (2005), pp. 4203–4215.

[8] E. J. Candès and T. Tao, *Near-optimal signal recovery from random projections: Universal encoding strategies*, IEEE Trans. Inform. Theory **52**, no. 12 (2006), pp. 5406–5425.

[9] S. S. Chen, D. L. Donoho, and M. A. Saunders, *Atomic decomposition by basis pursuit*, SIAM J. Sci. Comput. **20**, no. 1 (1999), pp. 33–61.

[10] O. Christensen, *An introduction to frames and Riesz bases*, Birkhäuser, Boston, (2003).

[11] A. Cohen, W. Dahmen, and R. DeVore, *Compressed sensing and best k-term approximation*. Preprint, RWTH Aachen, (2006).

[12] D. L. Donoho, *Compressed sensing*, IEEE Trans. Inform. Theory **52**, no. 4 (2006), pp. 1289–1306.

[13] D. L. Donoho, *For most large underdetermined systems of equations, the minimal $\ell_1$-norm near-solution approximates the sparsest near-solution*, Comm. Pure Appl. Math. **59**, no. 7 (2006), pp. 907–934.
[14] D. L. Donoho, *For most large underdetermined systems of linear equations the minimal $\ell_1$-norm solution is also the sparsest solution*, Comm. Pure Appl. Math. **59**, no. 6 (2006), pp. 797–829.
[15] D. L. Donoho and M. Elad, *Optimally sparse representation in general (nonorthogonal) dictionaries via $\ell^1$ minimization*, Proc. Natl. Acad. Sci. USA **100**, no. 5 (2003), pp. 2197–2202.
[16] D. L. Donoho, M. Elad, and V. Temlyakov, *Stable recovery of sparse overcomplete representations in the presence of noise*, IEEE Trans. Inform. Theory **52**, no. 1 (2006), pp. 6–18.
[17] D. L. Donoho and X. Huo, *Uncertainty principles and ideal atomic decomposition*, IEEE Trans. Inform. Theory **47**, no. 7 (2001), pp. 2845–2862.
[18] D. L. Donoho, Y. Tsaig, I. Drori, and J.L. Starck, *Sparse solution of underdetermined linear equations by stagewise orthogonal matching pursuit*, Tech. Report 2006-02, Standford, Department of Statistics, (2006).
[19] M. R. Garey and D. S. Johnson, *Computers and Intractability. A Guide to the Theory of NP-Completeness*, W. H. Freeman and Company, New York, (1979).
[20] S. Jokar and M. Pfetsch, *Exact and approximate sparse solutions of underdetermined linear equations*, SIAM J. Sci. Comput., to appear, (2008).
[21] N. Karmarkar, *A new polynomial-time algorithm for linear programming*, Combinatorica **4**, no. 4 (1984), pp. 373–395.
[22] L. G. Khachiyan, *A polynomial algorithm in linear programming*, Soviet Math. Dokl. **20** (1979), pp. 191–194.
[23] S. Kunis and H. Rauhut, *Random sampling of sparse trigonometric polynomials II – orthogonal matching pursuit versus basis pursuit*. Foundations of Computational Mathematics, to appear, (2007).
[24] B. K. Natarajan, *Sparse approximate solutions to linear systems*, SIAM J. Comput. **24**, no. 2 (1995), pp. 227–234.
[25] H. Rauhut, *Stability results for random sampling of sparse trigonometric polynomials*. Preprint, arXiv:math/0609630v2, (2006).
[26] H. Rauhut, *Random sampling of sparse trigonometric polynomials*, Appl. Comput. Harmonic Analysis **22**, no. 1 (2007), pp. 16–42.

## Large Deformations and Error Estimation

Arnd Meyer

The efficient fast solution of deformation problems using adaptive h-refined finite element approximation requires an appropriate mesh control. In linear elasticity this can be obtained from a residual error estimator in the following sense.

We consider the error functional

$$J_1(u-u_h) = a(u-u_h, u-u_h)^{1/2},$$

where u is the exact and $u_h$ the finite element soution. Here, $a(u,v)$ is the underlying bilinear form, such as

$$a(u,v) = \int_\Omega \sigma(u) : \epsilon(v)\ d\Omega$$

with small strain tensor $\epsilon$ and stress tensor $\sigma(u) = C : \epsilon(u)$ for some constant Hook's tensor C.

With the well-known techniques [1–3] we obtain

$$J_1(u-u_h) \leq const \cdot \left( \sum_{\forall T} \eta_T^2 \right)^{1/2}$$

with the element error contribution $\eta_T$ for the single element T of the actual finite element mesh. Hence, those elements with large contribution $\eta_T$ are marked for refinement, what leads to a very efficient adaptive approximation of the problem with a moderate number of unknowns.

The generalization of this approach to the more complicate case of geometrically nonlinear (large strain) deformations is now considered here.

We obtain a nonlinear weak formulation with

$$a(U;V) = \int_\Omega T_1(U) : GradV^T d\Omega = \int_\Omega T_2(U) : E(U;V)\ d\Omega.$$

Here, $T_1$ denotes the 1st Piola Kirchhoff stress tensor,

$T_2 = T_1 F^T$ the 2nd Piola Kirchhoff stress tensor and

$$E(U;V) = \frac{1}{2}(GradV + GradV^T + GradUGradV^T + GradVGradU^T)$$

occurs in linearizing the large strain tensor

$$E(U) = \frac{1}{2}(GradU + GradU^T + GradUGradU^T)$$

with the deformation gradient $F = I + GradU^T$ .

Now, different to the linear case, we have no energy norm (such as $a(u,u)$). The generalization of a residual type error estinator is based on a slight change of the error functional to

$$J_2(U-U_h) = \frac{a(U;U-U_h) - a(U_h;U-U_h)}{b(U-U_h,U-U_h)^{1/2}},$$

when $b(V,V)^{\frac{1}{2}}$ stands for a norm on V. An appropriate definition is:

$$b(U,V) = \int_\Omega \mathcal{E}(x)(GradV)^T : GradU\ d\Omega$$

with a "material size field" $\mathcal{E}(x)$. Note that in the linear case the definition $b(U,V) = a(U,V)$ leads to $J_1$.

Now, exactly the same techniques as for linear elasticity applied to $J_2$ leads to the error estimator:

$$J_2(U-U_h) \leq C_I(\sum \eta_T^2)^{1/2},$$

with the (small) constant $C_I$ from the interpolation estimates and with

$$\eta_T^2 = \frac{1}{\lambda_T}\left( h_T^2 \|r_T\|_{0,T}^2 + \sum_{E\subset\partial T} h_E \|r_E\|_{0,E}^2 \right).$$

Here, the element residual is $r_T = DivT_1 + f$ and $r_E$ are the edge jump terms again defined with $T_1(U_h)$ as: $r_E = [\mathfrak{n} \cdot T_1]$

Hence, the error estimator for large deformation coincides with its linear counterpart. The non–symmetric tensor $T_1$ occurs instead of the small–stress tensor.

### References

[1] R. Verfürht, *A review of aposterior error estimation and adaptive mesh-refinement techniques*, John Wiley & Sons, B. G. Teubner (1995)
[2] E. Stein (Eds.), *Error-controlled Adaptive Finite Elements in Solid Mechanics*, John Wiley & Sons (2003),(Sections 5 and 7)
[3] M. Ainsworth, J. T. Oden, *A Posteriori Error Estimation in Finite Element Analysis*, John Wiley & Sons (2000)

## A Software Infrastructure JASMIN for Parallel Adaptive Structured Mesh Applications

Zeyao Mo

This talk will introduce a software infrastructure JASMIN for large scale parallel adaptive structured mesh applications using thousands of processors. JASMIN is a software project for very large scale scientific computing supported by IAPCM and the National Basic Key Research Special Fund in China. It is developed to solve the more and more serious difficulties arising from the large scale parallel numerical simulations while the adaptive structured meshes are required and thousands of processors are used. These difficulties include the reduction of software complexities, the data structure for high performance, the simplification of parallel implementation, the fast algorithms and robust solvers, the visualization of large scale data set, and so on. The layered, modularized and object-oriented parallel programming techniques is used to design JASMIN. Three layers are provided. The basic layer includes the parallel adaptive implementations. In this layer, efficient data structure "hierarchy- level-patch-patch data" suitable for the high Cache hit ratio is used. Data communications and load balancing are organized and encapsulated. Mesh adaptivity operations are also encapsulated. Many useful programming tools are presented. In the middle layer, efficient time integration algorithms are integrated, robust solvers such as KINSOL and Hypre developed in LLNL are encapsulated, the description of the complex geometries are permitted. In the top layer, abstract interfaces based on the data structures such as patch and patchdata are presented, visualization tools are presented. Based on JASMIN, user is required to serially implement the abstract interfaces according to the physical models and the computational methods, then he will automatically get a parallel code which can efficiently run on the modern parallel computers using thousands of processors. Now, JASMIN is successfully applied to solve many realistic applications arising from the multi-material radiation hydrodynamics using various hydrodynamics methods such as the Euler, Lagrangian or Moving-Mesh, turbulence and interface instability simulation, laser plasma interactions using the Particle-In-Cell method, earth atmosphere environment simulation, material science using the molecular simulation, and so on. On a massively parallel computer, JASMIN can support many applications scaling up to 4096 processors.

## Exponential functionals of Brownian motion and class one Whittaker functions

Neil O'Connell
(joint work with Fabrice Baudoin, Toulouse)

If $(B_t^{(\mu)}, t \geq 0)$ is a standard one-dimensional Brownian motion with drift $\mu$,

$$\left( B_t^{(\mu)} + \log \left( \int_0^t e^{-2B_s^{(\mu)}} ds \right), t \geq 0 \right)$$

is a diffusion with generator given by

$$\frac{1}{2} \frac{d^2}{dx^2} + \left( \frac{d}{dx} \log K_\mu(e^{-x}) \right) \frac{d}{dx}.$$

This is a theorem of Matsumoto and Yor [8] and can be regarded as an extension of Pitman's '$2M - X$' theorem; the latter can be recovered by Brownian scaling and the method of Laplace. An interpretation of the law of this process as that of the Brownian motion with drift conditioned on the law of the exponential functional $\int_0^\infty \exp(-2B_t^{(|\mu|)})dt$ is given in [2]. We identify a class of diffusions which should play a similar role in a *multi-dimensional* version of this theorem, analogous to the multi-dimensional versions of Pitman's '$2M - X$' theorem obtained in [5, 6, 9]. As a starting point, we consider exponential functionals of a multi-dimensional Brownian motion with drift, defined via a collection of linear functionals. We give a characterisation of the Laplace transform of their joint law as the unique bounded solution, up to a constant factor, to a certain partial differential equation. We then consider a family of diffusions which can be interpreted as having the law of the Brownian motion with drift conditioned on the joint law of these exponential functionals. In the case where the collection of linear functionals is a set of simple roots, the Laplace transform of the joint law of the corresponding exponential functionals can be expressed in terms of a class one Whittaker function associated with the corresponding semi-simple Lie group. In this case, we study in detail some properties of the associated diffusion processes, which we call *Whittaker processes*. Class one Whittaker functions associated with semi-simple Lie groups have been studied extensively in the literature. They are closely related to Whittaker models of class one principal series representations and play an important role in the study of automorphic forms associated with semi-simple Lie groups [7]. In the integrable systems literature, they arise as eigenfunctions of the quantum Toda lattice [1].

### References

[1] V.I. Arnol'd and S.P. Novikov (Eds.), *Dynamical systems VII: Integrable systems, nonholonomic dynamical systems*, Encyclopaedia of Mathematical Sciences **16** (1994), Springer-Verlag, Berlin.

[2] F. Baudoin, *Further exponential generalization of Pitman's $2M - X$ theorem*, Electron. Comm. Probab. **7** (2002), 37–46.

[3] F. Baudoin, *Conditioned stochastic differential equations: Theory, Examples and Applications to Finance*, Stoch. Proc. Appl. **100** (2002), 109–145.

[4] F. Baudoin and N. O'Connell, *Exponential functionals of Brownian motion and class one Whittaker functions*, in preparation.
[5] Ph. Biane, Ph. Bougerol and N. O'Connell, *Littelmann paths and Brownian paths*, Duke Math. J. **130** (2005), no. 1, 127–167.
[6] Ph. Bougerol and T. Jeulin, *Paths in Weyl chambers and random matrices*, Probab. Theory Related Fields **124** (2002), no. 4, 517–543.
[7] D. Bump, *Automorphic Forms and Representations*, Cambridge University Press, 1998.
[8] H. Matsumoto and M. Yor, *A version of Pitman's* $2M - X$ *theorem for geometric Brownian motions*, C. R. Acad. Sci. Paris **328**, Série 1 (1999), 1067–1074.
[9] N. O'Connell and M. Yor, *A representation for non-colliding random walks*, Elect. Commun. Probab. **7** (2002), 1–12.

## Numerical Mathematics Aspects of Computational Finance

Cornelis W. Oosterlee

When valuing and risk-managing exotic derivatives, practitioners demand fast and accurate prices and sensitivities. As the financial models and option contracts used in practice are becoming increasingly complex, efficient methods have to be developed to cope with such models. Aside from non-standard exotic derivatives, plain vanilla options in many stock markets are actually of the American type. As any pricing and risk management system has to be able to calibrate to these plain vanilla options, it is important to be able to value these American options quickly and accurately.

By means of the risk-neutral valuation formula the price of any option without early exercise features can be written as an expectation of the discounted payo? of this option. Starting from this representation one can apply several numerical techniques to calculate the price itself: Monte Carlo simulation, numerical solution of the corresponding partial-(integro) differential equation (P(I)DE) and numerical integration. While the treatment of early exercise features within the first two techniques is relatively standard, the pricing of such contracts via quadrature pricing techniques has not been considered until recently, see [1, 9]. Each of these methods has its merits and demerits, though for the pricing of American options the PIDE approach currently seems to be the clear favourite.

In the past couple of years a vast body of literature has considered the modeling of asset returns as infinite activity Lévy processes, due to the ability of such processes to adequately describe the empirical features of asset returns and at the same time provide a reasonable fit to the implied volatility surfaces observed in option markets. Valuing American options in such models is however far from trivial, due to the weakly singular kernels of the integral terms appearing in the PIDE, as reported in, e.g., [2, 4, 6, 11].

In this presentation we present a quadrature-based method for pricing options with early exercise features. The method combines the recent quadrature pricing methods of [1] and [10] with the methods based on Fourier transformation pioneered by [3, 7, 8]. Though the transform methods so far have mainly been used for the pricing of European options, we show how early exercise features can be incorporated naturally. The requirements of the method are that the increments

of the driving processes are independent of each other, and that the conditional characteristic function of the underlying asset is known. This is certainly the case for many exponential Lévy models and models from the broader class of regular affine processes, which also encompasses the exponentially affne jump-diffusion class of [5]. In contrast to the PIDE methods, processes of infinite activity, such as the Variance Gamma (VG) or CGMY models can be handled with relative ease.

All transform methods start from the risk-neutral valuation formula that, for a European option, reads:

$$V(t, S(t)) = e^{-r\tau}\mathbb{E}[V(T, S(T))], \tag{1}$$

where $V$ denotes the value of the options, $r$ is the risk-neutral interest rate, $t$ is the current time point, $T$ is the maturity of the option and $\tau = T - t$. The variable $S$ denotes the asset on which the option contract is based. The expectation is taken with respect to the risk-neutral probability measure. As (1) is an expectation, it can be calculated via numerical integration provided that the probability density is known in closed-form. This is not the case for many models which do however have a characteristic function in closed form.

The best known examples of options with early exercise features are American and Bermudan options. American options can be exercised at any time prior to the option's expiry, whereas Bermudan options can only be exercised at certain dates in the future. We now define the set of exercise dates as $\mathcal{T} = \{t_1, \ldots, t_M\}$ and $0 = t_0 \leq t_1$. For the ease of exposure we assume the exercise date are equally spaced, so that $t_{m+1} - t_m = \Delta t$. If the option is exercised at some time $t \in \mathcal{T}$ the holder of the option obtains the exercise payoff $E(t, S(t))$. The Bermudan option price can then be found via backward induction as

$$\begin{cases} V(t_M, S(t_M)) &= E(t_M, S(t_M)) \\ C(t_m, S(t_m)) &= e^{-r\Delta t}\mathbb{E}_{t_m}\left[V(t_{m+1}, S(t_{m+1}))\right] \\ V(t_m, S(t_m)) &= \max\{C(t_m, S(t_m)), E(t_m, S(t_m))\}, \\ V(t_0, S(t_0)) &= C(t_0, S(t_0)), \end{cases} \quad m = M-1, \ldots, 1, \tag{2}$$

with $C$ the continuation value of the option and $V$ the value of the option immediately prior to the exercise opportunity. Note that we nw attached a subscript to the expectation operator to indicate that the expectation is being taken with respect to all information available at time $t_m$.

The dynamic programming problem in (2) is a successive application of the risk-neutral valuationi formula, as we can write the continuation value as

$$C(t_m, S(t_m)) = e^{-r\Delta t}\int_{-\infty}^{+\infty} V(t_{m+1}, y) f(y|S(t_m))dy, \tag{3}$$

where $f(y|S(t_m))$ represents the probability density describing the transition from $S(t_m$ at $t_m$ to $y$ at $t_{m+1}$. The previous literature does not seem to have picked up on a presentation by Reiner [10], where it was recognised that for a Black-Scholes model the risk-neutral valuation formula in (3) can be seen as a convolution or

correlation of the continuation values with the transition density. As convolutions can be handled very efficiently by means of the FFT, an overall complexity of $O(MN\log_2 N)$ can be achieved.

As one of the defining properties of a Lévy process is that its increments are independent of each other, the insight of Renier has a much wider applicability than only to the Black-Scholes model. This is especially appealing since the usage of Lévy processes in finance has become more stablished nowadays. By combining Reiner's ideas with the work of Carr and Madan, we introduce the Convolution method, or CONV method for short. The complexity of the method is $O(MN\log_2 N)$ for an $M$-times exercisable option.

Our method has similarities with both the quadrature pricing and the PIDE methods. However, our application of the FFT to approximate convolution integrals bears more resemblance to the approximation of the integral term in the numerical solution of a PIDE.

## References


[1] A. D. Andricopoulos, M. Widdicks, P. W. Duck and D. P. Newton *Universal Option Valutation Using Quadrature,* J. Finantial Economics*, vol. 67(3), 447–471, 2004*

[2] A. Almendral and C. W. Oosterlee, *On American options under the Variance Gamma process,* Applied Math. Finance*, vol. 14(2), 131–152, 2007*

[3] P. P. Carr and D. B. Madan, *Option valuation using the Fast Fourier Transform,* J. Comp. Finance*, vol. 2, 61–73, 1999*

[4] R. Cont and P. Tankov *Financial modelling with jump processes, Chapman and Hall, Boca Raton, FL. 2004*

[5] D. Duffie, J. Pan, and K. Singleton *Transfor analysis and asset pricing for affine jump-diffusions,* Econometrica*, vol. 68, 1343–1376, 2000*

[6] A. Hirna and D. B. Madan *Pricing American Options Under Variance Gamma,* J. Comp. Finance*, vol. 7, 2004*

[7] A. Lewis *A simple option formula for general jump-diffusion and other exponential Lévy processes. SSRN working paper, 2001. Available at: hppt//ssrn.com/abstracts-282110.*

[8] S. Raible Lévy processes in Finance: Theory, Numerics and Empirical Facts*. PhD Thesis Inst. für Math. Stochasitk, Albert-Ludwigs-Univ. Freiburg, 2000*

[9] E. Reiner Convolution Methods for Path-Dependent Options*, Financial Math. workshop, IPAM UCLA, Jan. 2001, Available through http : //www.ipam.ucla.edu/publications/fm2001/fm2001*$_4$*272.pdf*

[10] C. O'Sullivan Path Dependent Option Pricing under Lévy Processes *EFA 2005 Moscow Meetings Paper, Available at SSRN: http://sern.com/abstract=673424, Febr. 2005*

[11] I. Wang, J. W. Wan and P. Forsyth *Robust numerical valuation of European and American options under the CGMY process.* J. Computational Finance*, 10(4), 31–70, 2007*

## Proving $H^{1+\alpha}$ Bernstein inequalities for non-nested multilevel spaces

Peter Oswald

Non-nestedness $V_{j-1} \not\subset V_j$ in multiscale ladders of discretization spaces $\{V_j\}_{j\geq 0}$ appears naturally (non-conforming finite-element discretizations, constrained discretizations such as discretely divergence-free discretizations for incompressible flow, multilevel partition of unity methods, etc.), and leads to some technical difficulties from the point of view of multigrid theory. In non-nested situations, the additional degree of freedom is the choice of appropriate coarse-to-fine prolongation operators, and the main difficulty to control the perturbations introduced by their recursive appearance in multiscale algorithms. Bramble et al. (see the monograph [1]) have made a first attempt to develop a generic theory, it guarantees W-cycle optimality with sufficiently many smoothing steps, and variable V-cycle optimality. Later Brenner [2,3] was able to cover V-cycle and F-cycle multigrid methods with sufficiently many smoothing steps. Independently, the author obtained suboptimality results for additive Schwarz multilevel preconditioners for standard nonconforming finite element discretizations [4,8] by proving uniform energy norm bounds for *iterated* prolongation operators $P_{\ell\to j} = P_j \cdots P_{\ell+1} : V_\ell \to V_j$. Other approaches such as the "switching" procedure (i.e., mapping to a nested hierarchy of discretization spaces by a two-level method) have been developed as well.

The case most resistent to theoretical treatment is the analysis of Schwarz-type multilevel preconditioners and V-cycle algorithms with one or two smoothing steps, where perturbations coming from the prolongations may not be sufficiently damped by smoothing. In [9] we recently solved a particular instance of this open problem by showing optimality of a hierarchical basis preconditioner for non-conforming P1 elements proposed in [7]. The last step of improving the $O(J)$ condition number bound from the original 1992 paper [7] to the optimal $O(1)$ bound is based on a discrete $H^{1+\alpha}$ Bernstein inequality involving the iterated prolongation operators for some $\alpha > 0$. For proving such Bernstein inequalities, ideas borrowed from the theory of semi-regular subdivision methods were essential (for a survey of this class of multiscale algorithms with applications to geometric modeling, see [5]). In the terminology of the latter, our result is equivalent to proving $H^{1+\alpha}$ regularity of the limit surfaces of the subdivision scheme generated by the prolongations. This in turn requires the consideration of local subdivision operators for a finite number of so-called invariant neighborhoods which for two-dimensional triangular meshes are associated with regular triangles, extraordinary interior vertices of valence $\neq 6$, and boundary edges and vertices (in [9] we have opted to treat the boundary by an alternative extension trick), and the study of their spectral properties. In the particular case of the standard prolongation operators for nonconforming P1 elements (obtained by averaging the two-sided limits at discontinuity points located on coarse edges), we showed that the Sobolev regularity of the limit surfaces near regular triangles equals $s_2 = 1.2838\ldots$, and that near extraordinary vertices it stays $> 1$ for all valences. This is sufficient to conclude the uniform upper spectral bound for the associated multilevel preconditioner.

The methodology of this case study is more widely applicable, at least, it easily extends to non-nested discretizations of symmetric positive-definite elliptic problems of order $0 < k < 3$. In [6], we applied it to $\sqrt{3}$-refined triangular meshes and discretizations of Laplace-type problems. $\sqrt{3}$-refinement has the advantage of a slower growth of the dimensions of discretized problems (with factor $\sim 3$ rather than factor $\sim 4$ for standard quadrisection), and additionally offers an improved directional selectivity. The paper [6] also elaborates on how to prove lower bounds for the spectrum of the associated multilevel preconditioner for general prolongations.

Another (so far only experimentally supported) insight we gained is that the performance of multilevel preconditioners in the pre-asymptotic range depends on the prolongation operators essentially through the actual size of the spectral radii of the iterations of a transfer operator associated with the involved local subdivision operators. This has lead us to the construction of a new prolongation operator for non-conforming P1 element discretizations with improved preconditioning power in both the asymptotic and pre-asymptotic range [10]. In comparison with the standard prolongation, the calculated limit Sobolev smoothness of $s_2 = 1.6165\ldots$ for the associated subdivision method near regular triangles is considerably higher.

Future research will focus on higher-order elliptic problems (e.g., 4-th order elliptic problems and non-nested discretely divergence-free Stokes discretizations), and three-dimensional situations, where more complex local mesh topologies become a major challenge.

## References


[1] J. Bramble, *Multigrid Methods*, Pitman Research Notes in Math., vol. 294, Longman, London, 1993.

[2] S. Brenner, *Convergence of nonconforming multigrid methods without full elliptic regularity*, Math. Comp. **68** (1999), 25–53.

[3] S. Brenner, *Convergence of the multigrid V-cycle algorithms for second order boundary value problems without full elliptic regularity*, Math. Comp. **71** (2002), 507–525.

[4] Z. Chen, P. Oswald, *Multigrid and multilevel methods for nonconforming Q1 elements*, Math. Comp. **67** (1998), 667–693.

[5] N. Dyn, D. Levin, *Subdivision schemes in geometric modelling*, Acta Numerica (2002), 73–144.

[6] J. Maes, P. Oswald, *Multilevel finite element preconditioning for $\sqrt{3}$ refinement*, Math. Comp. (submitted 2007, under revision).

[7] P. Oswald, *On a hierarchical basis multilevel method with nonconforming P1 elements*, Numer. Math. **62** (1992), 189–212.

[8] P. Oswald, *Intergrid transfer operators and multilevel preconditioners for nonconforming discretizations*, Appl. Numer. Meth. **23** (1997), 139–158.

[9] P. Oswald, *Optimality of multilevel preconditioning for nonconforming P1 finite elements*, Numer. Math. (submitted 2007).

[10] P. Oswald, *Optimized prolongation operators for nonconforming P1 element multilevel preconditioners* (in preparation).

## Recent advances in Composite Finite Elements

Daniel Peterseim
(joint work with Stefan A. Sauter)

Many physical processes that can be modeled by partial differential equations such as groundwater or ocean flows take place in complex environments (shore lines are rarely smooth). Finite element methods are known to be very powerful tools in the numerical investigation of such processes. In principle, the concept of finite elements is sufficient to handle problems on complicated domains, but the standard requirement saying that the underlying finite element mesh has to resolve the boundary of the physical domain is too restrictive if the domain contains small geometric details such as rough boundaries or holes. The resolution condition links the number of elements to the number (and size) of geometric details. Therefore, the minimal dimension of the approximation space reaches a size which is not feasible to solve with a standard computer. Neither can spaces based on resolving grids serve as coarse grid spaces in multilevel solvers. In practice, one is often interested in a moderate accuracy that cannot be achieved at a moderate effort if the mesh has very fine parts used to resolve the geometry. Furthermore, the mesh density of coarse shape regular triangulations of complicated domains is determined by the geometry and *not* by the smoothness properties of the solution.

To be more precise, consider the simple setting of the Poisson equation $-\Delta u = f$ on a polyhedral domain $\Omega \subset \mathbb{R}^2$ having $N_\Omega$ sides. In case of Dirichlet boundary condition the discrete weak variational problem reads

$$\int_\Omega \nabla u \cdot \nabla v = \int_\Omega fv, \quad \forall v \in V, \tag{1}$$

where $V = V_{\mathcal{T}} \subset H_0^1(\Omega)$ contains typically continuous piecewise polynomials with respect to some regular triangulation $\mathcal{T}$ of $\Omega$. The a priori error for a piecewise

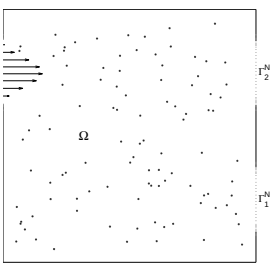


(a) Model domain $\Omega$ with tiny holes.

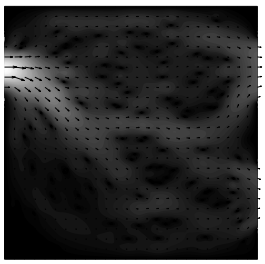

(b) Solution velocity (black= 0, white= 1).

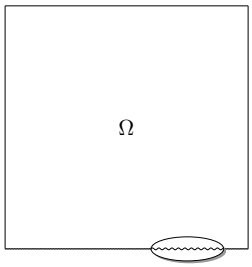


(c) Model domain $\Omega$ with oscillating bottom boundary.

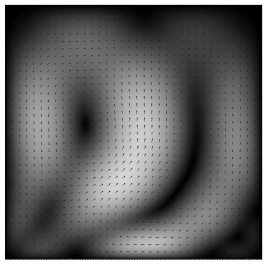

(d) Solution velocity (black= 0, white= 0.5).

Figure 1. Model problems: (a-b) Stokes flow on the unit square with 100 tiny holes, a Dirichlet inflow boundary and two Neumann outflow boundaries. (c-d) Force driven Stokes flow in a domain with rough slip bottom boundary.

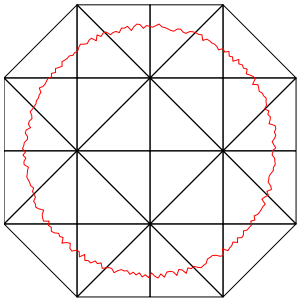

(a) Initial coarse triangulation.

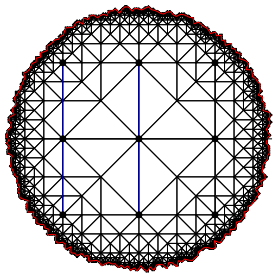

(b) Structured refinement of triangulation in 2a, degrees of freedom (•).

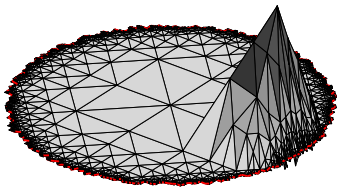

(c) Composite basis function (fulfills the Dirichlet boundary condition in an approximative way).

FIGURE 2. Structured overlapping triangulation of a two dimensional domain with a rough boundary and composite finite element basis function.

linear finite element approximation $u_{\mathcal{T}} \in V$ can be estimated by

$$\|u - u_{\mathcal{T}}\| \lesssim \inf_{v \in V} \|u - v\|_{H^1(\Omega)} \lesssim h^r |u|_{H^{1+r}(\Omega)}, \tag{2}$$

where $h$ denotes the maximal meshwidth of $\mathcal{T}$ and $r \in (\frac{1}{2}, 1]$. The crucial condition for this estimate in case of $N_\Omega$ large is the so called conformity condition $V \subset H_0^1(\Omega)$ since it demands $\mathcal{T}$ to be exact. No matter which accuracy one is interested in, the dimension of $V$ is always bounded from below by $N_\Omega$. The resulting linear system might be too large to be solved efficiently. The situation can be even worse in three space dimensions where mesh generation is still a bottle neck in many cases. Overlapping triangulations $\mathcal{T}$ (cf. Figure 2a) allow the definition of low dimensional approximation spaces, but the resulting approximation error will be reflected truly by the sum

$$\inf_{v \in V} \|u - v\|_{H^1(\Omega)} + \sup_{v \in V \setminus \{0\}} \frac{\|v\|_{L^2(\partial\Omega)}}{\|v\|_{H^1(\Omega)}}.$$

While the infimum still can be estimated in terms of the maximal mesh width $h$, the supremum has a negative effect (pollution) on the overall approximation. To overcome this problem we define coarse finite element spaces (cf. [4]) that preserve the a priori bound given in (2) without the crucial coupling between domain geometry and space dimension. This work bases on the concept of composite finite elements introduced by Hackbusch and Sauter (cf. [2], [3]). Starting from a possibly coarse, overlapping triangulation (cf. Figure 2a) all triangles that intersect the boundary are refined successively (cf. Figure 2b). Note, that the number of refinement steps does not depend on the complicated geometry but only on the meshwidth $h$ of the initial grid. Additionally, the degrees of freedom are the same

as in the initial coarse triangulation. New nodes do not enlarge the space dimension, since they become slave nodes. Composite shape functions $u^{\mathrm{cfe}}$ are defined by mapping shape functions $u$ according to the initial triangulation to the finite element space with respect to the refined triangulation. The (linear) mapping is explicitly given by the simple formula

$$u^{\mathrm{cfe}}(x) = \begin{cases} u(x), & x \text{ interior node} \\ u(x) - u(x^{\partial\Omega}), & \text{else,} \end{cases} \tag{3}$$

where $x^{\partial\Omega}$ denotes an (approximative) projection of $x$ to the boundary of $\Omega$. A typical basis function of the resulting space $V^{\mathrm{cfe}}$ is depicted in Figure 2c. The dimension of the composite space $V^{\mathrm{cfe}}$ does *not* depend on $N_\Omega$. Apart from this result, the composite finite element approximation fulfills an a priori error bound which is optimal in the meshwidth parameter $h$ (cf. [5]):

$$\|u - u^{\mathrm{cfe}}\| \lesssim h^r |u|_{H^{1+r}(\Omega)}.$$

The estimate remains true for Lipschitz domains in two as well as three space dimensions (cf. [4] and [1]). Recently, the concept of composite finite elements has further been extended to Stokes problem with mixed Dirichlet, Neumann, slip and leak boundary conditions (cf. [4], [1]). It allows to compute Stokes flows with reasonable accuracy with only a few degrees of freedom. In many cases (see for instance Figure 1) their number can be chosen much smaller than the number of geometric details ($N_\Omega$).

## References


[1] Peterseim, D. and Sauter, S. A., *The Composite Mini Element: Coarse mesh computation of Stokes flows on complicated domains*, to appear in Siam J. Num. Anal.

[2] Hackbusch, W. and Sauter, S. A., *Composite finite elements for the approximation of PDEs on domains with complicated micro-structures*, Numer. Math., **75(4)** (1997), 447–472.

[3] Hackbusch, W. and Sauter, S. A., *Composite finite elements for problems containing small geometric details. Part II: Implementation and numerical results*, Computing and Visualization in Science **1** (1997), 15–25.

[4] Peterseim, D. *The Composite Mini Element: A mixed FEM for the Stokes equations on complicated domains*, Dissertation, Universität Zürich (2007).

[5] Rech, M., Sauter, S. and Smolianski, A., *Two-scale composite finite element method for Dirichlet problems on complicated domains*, Numer. Math. **102 (4)** (2006), 681–708.


## Numerical methods for two-phase incompressible flows


Arnold Reusken

(joint work with Maxim Olshanskii)


Let $\Omega \subset \mathbb{R}^3$ be a polyhedral domain containing two different immiscible incompressible phases. The time dependent subdomains containing the two phases are denoted by $\Omega_1(t)$ and $\Omega_2(t)$ with $\bar{\Omega} = \bar{\Omega}_1 \cup \bar{\Omega}_2$ and $\Omega_1 \cap \Omega_2 = \emptyset$. We assume that $\Omega_1$ and $\Omega_2$ are connected and $\partial\Omega_1 \cap \partial\Omega = \emptyset$ (i. e., $\Omega_1$ is completely contained in $\Omega$). The interface is denoted by $\Gamma(t) = \bar{\Omega}_1(t) \cap \bar{\Omega}_2(t)$. A typical example is a rising air bubble or liquid droplet in a surrounding fluid. The standard model for

describing incompressible two-phase flows consists of the Navier-Stokes equations in the subdomains with the coupling condition

$$[\boldsymbol{\sigma}\mathbf{n}]_\Gamma = \tau\mathcal{K}\mathbf{n} \tag{1}$$

at the interface, i. e., the surface tension balances the jump of the normal stress at the interface. The surface tension coefficient $\tau$ is assumed to be constant. We use the notation $[v]_\Gamma$ for the jump of $v$ across $\Gamma$, $\mathbf{n} = \mathbf{n}_\Gamma$ is the unit normal at the interface $\Gamma$ (pointing from $\Omega_1$ into $\Omega_2$), $\mathcal{K}$ the curvature of $\Gamma$ and $\boldsymbol{\sigma}$ the stress tensor defined by $\boldsymbol{\sigma} = -p\mathbf{I} + \mu\mathbf{D}(\mathbf{u})$ with $\mathbf{D}(\mathbf{u}) = \nabla\mathbf{u} + (\nabla\mathbf{u})^T$. Furthermore $p = p(\mathbf{x}, t)$ denotes the pressure, $\mathbf{u} = \mathbf{u}(\mathbf{x}, t)$ the velocity and $\mu$ the viscosity. We assume continuity of $\mathbf{u}$ across the interface. Based on the conservation laws for mass and momentum the fluid dynamics is modeled by the Navier-Stokes equations in the two subdomains combined with $[\mathbf{u}]_\Gamma = 0$ and the coupling condition in (1), cf. for example [8, 11]. A level set method can be used for capturing the unknown interface, cf. [7, 9, 10]. The level set function, denoted by $\phi = \phi(\mathbf{x}, t)$ is a scalar function with $\phi(\mathbf{x}, 0) < 0$ for $\mathbf{x} \in \Omega_1(0)$, $\phi(\mathbf{x}, 0) > 0$ for $\mathbf{x} \in \Omega_2(0)$, $\phi(\mathbf{x}, 0) = 0$ for $\mathbf{x} \in \Gamma(0)$. It is desirable to have the level set function at $t = 0$ as an approximate signed distance function.

The evolution of the interface is given by the linear hyperbolic partial differential equation $\phi_t + \mathbf{u} \cdot \nabla\phi = 0$ for $t \geq 0$ and $\mathbf{x} \in \Omega$.

The jumps in the coefficients $\rho$ and $\mu$ can be described using the level set function (which has its zero level set precisely at the interface $\Gamma$) in combination with the Heaviside function $H$. We define

$$\begin{aligned} \rho(\phi) &:= \rho_1 + (\rho_2 - \rho_1)H(\phi), \\ \mu(\phi) &:= \mu_1 + (\mu_2 - \mu_1)H(\phi). \end{aligned} \tag{2}$$

The effect of the surface tension can be expressed in terms of a localized force at the interface, cf. the so-called continuum surface force (CSF) model [2,7]. Combination of the CSF approach with the level set method leads to the following model for the two-phase problem in $\Omega \times [0, T]$

$$\rho(\phi)\Big(\frac{\partial\mathbf{u}}{\partial t} + (\mathbf{u} \cdot \nabla)\mathbf{u}\Big) = -\nabla p + \rho(\phi)\mathbf{g} + \operatorname{div}(\mu(\phi)\mathbf{D}(\mathbf{u})) + \tau\mathcal{K}\delta_\Gamma\mathbf{n}_\Gamma \tag{3}$$

$$\operatorname{div}\mathbf{u} = 0 \tag{4}$$

$$\phi_t + \mathbf{u} \cdot \nabla\phi = 0 \tag{5}$$

together with suitable initial and boundary conditions for $\mathbf{u}$ and $\phi$. This is the continuous problem that we use to model our two-phase flow problem. It is also used in, for example, [7, 11, 12].

We formulate this problem in an appropriate weak form and use finite element techniques for discretization, cf. [3, 12]. We briefly address the weak formulation of the localized surface tension force. The surface tension term in (3) results in the functional

$$f_\Gamma(\mathbf{v}) := \tau \int_\Gamma \mathcal{K}\mathbf{n}_\Gamma \cdot \mathbf{v}\, \mathrm{d}\mathbf{s}, \quad \mathbf{v} \in \mathbf{V} := H_0^1(\Omega)^3. \tag{6}$$

The approximation of this localized surface tension force is based on the following Laplace-Beltrami characterization of the curvature. Let $\mathrm{id}_\Gamma : \Gamma \to \mathbb{R}^3$ be the identity on $\Gamma$ and $\mathcal{K} = \kappa_1 + \kappa_2$ the sum of the principal curvatures. For all sufficiently smooth vector functions $\mathbf{v}$ on $\Gamma$ the following holds:

$$f_\Gamma(\mathbf{v}) = \int_\Gamma \mathcal{K}\,\mathbf{n}_\Gamma \cdot \mathbf{v}\,\mathrm{d}\mathbf{s} = -\int_\Gamma (\Delta_\Gamma\,\mathrm{id}_\Gamma)\cdot\mathbf{v}\,\mathrm{d}\mathbf{s} = \int_\Gamma \nabla_\Gamma\,\mathrm{id}_\Gamma \cdot \nabla_\Gamma \mathbf{v}\,\mathrm{d}\mathbf{s}. \tag{7}$$

In [4] we introduced and analyzed the following discretization method for the surface tension force. Define

$$\tilde{\mathbf{n}}_h(\mathbf{x}) := \frac{\nabla\phi_h(\mathbf{x})}{\|\nabla\phi_h(\mathbf{x})\|}, \qquad \tilde{\mathbf{P}}_h(\mathbf{x}) := \mathbf{I} - \tilde{\mathbf{n}}_h(\mathbf{x})\tilde{\mathbf{n}}_h(\mathbf{x})^T, \quad \mathbf{x}\in\Gamma_h,\ \mathbf{x} \text{ not on an edge.}$$

Here $\Gamma_h$ is a polyhedral approximation of $\Gamma$ that is obtained as the zero level of an iso$P_2$ approximation of the piecewise quadratic approximate level set function $\phi_h$. The discrete surface tension force is given by

$$f_{\Gamma_h}(\mathbf{v}_h) = \tau \sum_{i=1}^{3} \int_{\Gamma_h} \tilde{\mathbf{P}}_h(\mathbf{x})\mathbf{e}_i \cdot \nabla_{\Gamma_h}(\mathbf{v}_h)_i\,\mathrm{d}\mathbf{s}, \tag{8}$$

with $\mathbf{e}_i$ the $i$-th basis vector in $\mathbb{R}^3$ and $(\mathbf{v}_h)_i$ the $i$-th component of $\mathbf{v}_h$.

The implementation of this functional requires the numerical integration over the triangulated surface $\Gamma_h = \cup_{T\in\mathcal{F}_h} T$ of functions that are smooth on the planar segments $T$ this triangulation.

In many two-phase flow systems surface active agents (surfactants) are present as impurities or added to the bulk fluid. To describe the effect of such surfactants a convection-diffusion equation *at* the interface is added to the fluid dynamics model (3)-(5). Let the velocity field $\mathbf{u}$ be decomposed in a tangential and normal component: $\mathbf{u} = \mathbf{u}_\Gamma + u_\perp \mathbf{n}$. Let $D_\Gamma > 0$ be a given diffusion coefficient of $\Gamma$. The following type of transport equation for the surfactant concentration $c = c_\Gamma$ can be found in the literature, cf. [1]:

$$\partial_{t,n} c - D_\Gamma \Delta_\Gamma c + \nabla_\Gamma \cdot (c\mathbf{u}_\Gamma) - \mathcal{K} u_\perp c = 0, \tag{9}$$

where $\partial_{t,n} c$ denotes the derivative of $c$ along a purely normal path. In case of a soluble surfactant a source term is added that describes the process of ad- and desorption of the surfactant. The flow field $\mathbf{u}$ results from the fluid dynamics model (3)-(5).

We present a new finite element approach for the discretization of elliptic partial differential equations on surfaces, cf. [6]. The main idea is to use finite element spaces that are induced by triangulations of an "outer" domain to discretize the partial differential equation on the surface. The method is particularly suitable for problems in which there is a coupling with a flow problem in an outer domain that contains the surface, for example, two-phase incompressible flow problems. In [6] it is proved that this method has optimal order of convergence both in the $H^1$ and in the $L^2$-norm. Results of numerical experiments illustrate this optimality. The coupling of this technique with the two-phase flow solver is discussed.

## References

[1] D. Bothe, J. Prüss and G. Simonett, *Well-posedness of a two-phase flow with soluble surfactant*, Progress in Nonlinear Differential Equations And Their Applications **64** (2005), 37–62.

[2] J. U. Brackbill, D. B. Kothe, C. Zemach, *A continuum method for modeling surface tension*, J. Comput. Phys. **100** (1992), 335–354.

[3] S. Groß, V. Reichelt and A. Reusken, *A Finite Element Based Level Set Method for Two-Phase Incompressible Flows*, J. Comp. Vis. Sci. **9** (2006),239–257.

[4] S. Groß and A. Reusken, *Finite element discretization error analysis of a surface tension force in two-phase incompressible flows*, SIAM J. Numer. Anal. **45** (2007), 1679–1700.

[5] S. Groß and A. Reusken, *An extended pressure finite element space for two-phase incompressible flows*, J. Comp. Phys. **224** (2007), 40–58.

[6] M. Olshanskii, A. Reusken and J. Grande, *An Eulerian Finite Element Method for elliptic equations on moving surfaces*, submitted to SIAM J. Numer. Anal. 2008.

[7] S. Osher, R. P. Fedkiw, *Level set methods: An overview and some recent results*, J. Comput. Phys. **169** (2001), 463–502.

[8] S. B. Pillapakkam, P. Singh, *A level-set method for computing solutions to viscoelastic two-phase flow*, J. Comput. Phys. **174** (2001), 552–578.

[9] J. A. Sethian, *Theory, algorithms, and applications of level set methods for propagating interfaces*, Acta Numerica **5** (1996), 309–395.

[10] J. A. Sethian, *Level set methods and fast marching methods*, Cambridge University Press, 1999.

[11] M. Sussman, A. S. Almgren, J. B. Bell, Ph. Colella, L. H. Howell, M. L. Welcome, *An adaptive level set approach for incompressible two-phase flows*, J. Comp. Phys. **148** (1999), 81–124.

[12] A.-K. Tornberg, B. Engquist, *A finite element based level-set method for multiphase flow applications*, Comput. Visual. Sci. **3** (2000), 93–101.


## Eulerian-Lagrangian Methods for Multiphase flows

Thomas Russell

Eulerian-Lagrangian methods (ELMs, also called "semi-Lagrangian", "characteristic Galerkin", etc. ) have been very successful in modeling many types of problems, including scalar convection-diffusion equations. It has not been clear how to extend these schemes to complicated systems of convection-dominated PDEs, in which the behavior of the dominant hyperbolic system could be problematic. This talk discusses a conceptual breakthrough in understanding how to make this extension for models of multiphase flows in the subsurface, such as compositional petroleum reservoir simulation or transport of groundwater, nonaqueous-phase phase liquid (NAPL) contaminants, and volatile organic compounds (VOCs). Such methods promise to improve the efficiency and accuracy of these simulations –reduced numerical diffusion, reduced nonphysical oscillations, obtainable with coarser grids and larger time steps than are possible with methods in current use. We first present background that motivates an operator-splitting approach on the basis of decomposing the system into weakly coupled subsystems, such that the couplings can be neglected within a Newon iteration, while the couplings are restored when the Newton residual is driven to zero. Lagrangian transport is relatively weakly coupled to the other processes in the system. Then we summarize the history of ELMs and present the Eulerian-Lagrangian localized adjoint method (ELLAM),

which applies its Lagrangian tracking to the adjoint (dual) of the original (primal) system. We show that, in contrast to the primal (wave-oriented) equation, the dual equations are viewed naturally in terms of movement of masses, volumes, or finite particles, and vecause these equations are linear, then characteristics do not cross and are always well-defined. The physical picture of movement of multiple fluids is directly reflected in the mathematical representation, thus also guiding the design of the numerical scheme. We present a simple shock propagation and a 1-D Buckley-Leverett example to illustrate the concept, including the manner in which both mass and volume can be properly conserved.

## Finite Volume/DG Schemes Based on Constrained Minimization Function Recovery

Panayot S. Vassilevski

ABSTRACT

In this talk we give an outline on the construction of finite volume/discontinuous Galerkin (FV/DG) schemes for the equations of gas dynamics in Lagrangian coordinates. The schemes utilize non–oscillatory smooth function recovery procedures. The recovery procedures are formulated as total variation (TV) functional minimization subject to constraints. The constraints have physical meaning, namely non-negativity of the internal energy (or pressure). We touch upon the implementation of the schemes and present some preliminary test results. A main task in the implementation is the solution of the nonlinear constrained minimization problems coupled with the multilevel local refinement involved in the non–oscillatory smooth function recovery. More details are found in the preliminary report [3].

### 1. The equations of gas dynamics in Eulerian and Lagrangian coordinates

1.1. **The equation of gas dynamics in Eulerian coordinates.** The Euler equations for a compressible inviscid fluid (where the heat conduction is neglected) can be written in the following conservative form (cf., e.g. [1]):

$$\begin{aligned} \frac{\partial \varrho}{\partial t} &= -\operatorname{div}(\varrho\, \mathbf{v}), \\ \frac{\partial(\varrho\, \mathbf{v})}{\partial t} &= -\nabla p - \sum_{j=1}^{d} \frac{\partial(\varrho v_j\, \mathbf{v})}{\partial x_j}, \\ \frac{\partial(\varrho\, E)}{\partial t} &= -\operatorname{div}\ ((\varrho\, E + p)\mathbf{v})\,. \end{aligned} \tag{1.1}$$

Here, $\varrho$ is the density of the fluid, $\mathbf{v} = (v_1, \ldots, v_d)$ is the fluid velocity, $p$ is the pressure, $e$ is the specific (per unit mass) internal energy, and $E = e + \frac{1}{2}\,|\mathbf{v}|^2$ is the specific (per unit mass) total energy. The equations in (1.1) describe the laws of conservation of mass, momentum, and total energy of the fluid. There is one

more equation, referred to as equation of state (or E.O.S.) associated with (1.1) that specifies the pressure $p$. In general it has the form

$$p = p(\varrho,\ e) = \mathrm{EOS}(\varrho,\ e),$$

which in the case of polytropic ideal gas reads $p = (\gamma - 1)\ \varrho e,$ for a constant $\gamma > 1$.

1.2. **The equations of gas dynamics in Lagrangian coordinates and their integral form.** Here, we present the equations of gas dynamics in Lagrangian coordinates in somewhat more general form than is traditionally used with the purpose to be used in the derivation of higher order DG schemes. The derivation is based on [1] (see [3]).

1.2.1. *Lagrangian coordinates.* Let $\mathbf{v} = \mathbf{v}(\mathbf{x},\ t)$ be the velocity field of the fluid flow. We consider the dynamical system $\frac{d\mathbf{x}}{dt} = \mathbf{v}(\mathbf{x},\ t)$ with initial condition $\mathbf{x}|_{t=0} = \boldsymbol{\xi}$. Consider the mapping $\boldsymbol{\xi} \mapsto$ the solution $\mathbf{x}(\boldsymbol{\xi},\ t)$ of the initial value problem. By definition, the pair $(\boldsymbol{\xi},\ t)$ is called Lagrangian coordinates associated with the velocity field $\mathbf{v}$.

1.2.2. *Integral form of the equations.* For a given multi-index $\underline{\alpha} = (\alpha_i)_{i=1}^d$, denote $\mathbf{x}^{\underline{\alpha}} = \prod_{i=1}^{d} x_i^{\alpha_i}$. For any given cell $V = V(t)$, we have the following integral form of the conservation of mass:

$$\frac{\partial}{\partial t} \int\limits_{V(t)} \mathbf{x}^{\underline{\alpha}}\ \varrho\ d\,\mathbf{x} = 0. \tag{1.2}$$

The integral form of the conservation of momentum equation reads

$$\frac{\partial}{\partial t} \int\limits_{V(t)} \mathbf{x}^{\underline{\alpha}}\ \varrho\mathbf{v}\ d\,\mathbf{x} = -\int\limits_{V(t)} \mathbf{x}^{\underline{\alpha}}\ \nabla p\ d\,\mathbf{x}. \tag{1.3}$$

The energy conservation equation has the following integral form

$$\frac{\partial}{\partial t} \int\limits_{V(t)} \mathbf{x}^{\underline{\alpha}}\ \varrho\ E\ d\mathbf{x} = -\int\limits_{V(t)} \mathbf{x}^{\underline{\alpha}}\ \mathrm{div}\ (p\mathbf{v})\ d\mathbf{x}. \tag{1.4}$$

The more general formulas (with $\underline{\alpha} \neq 0$) are the basis for deriving higher order DG schemes. However, in what follows we let $\underline{\alpha} = 0$.

## 2. Smooth function recovery from averages

Given an initial set of primal cells $V = V(0) \in \mathcal{T}_H$, introduce time discretization $t_{n+1} = t_n + \Delta t$ and let $V_n = V(t_n)$, $V_{n+1} = V(t_{n+1})$. From (1.2), we obtain that the mass $m(V_n) = \int\limits_{V(t_n)} \varrho\ d\ \mathbf{x} = Const.$ Thus, approximating the density with

piecewise constants, gives $\varrho_n = \frac{m(V)}{|V_n|}$ where $|V_n| = \int\limits_{V_n} 1 \, d\mathbf{x}$. Discretizing (1.3) as

$$\frac{m(V)}{\Delta t} \left( \frac{1}{|V_{n+1}|} \int\limits_{V_{n+1}} \mathbf{v} \, d\mathbf{x} - \frac{1}{|V_n|} \int\limits_{V_n} \mathbf{v} \, d\mathbf{x} \right) = - \int\limits_{V_n} \nabla p \, d\mathbf{x}$$

shows that the cell-averages $\frac{1}{|V_{n+1}|} \int\limits_{V_{n+1}} \mathbf{v} \, d\mathbf{x}$ are computable. Thus, we end up with the following problem of function recovery that is central to our schemes. Given the average values, we want to construct a smooth function $\mathbf{v}_h$ (that has the prescribed averages) to be used in the approximation of the conservation of energy equation

$$\frac{1}{\Delta t} \left( \int\limits_{V_{n+1}} \varrho \, e \, d\mathbf{x} - \int\limits_{V_n} \varrho \, e \, d\mathbf{x} \right) = - \int\limits_{V_{n+1}} p \, \mathrm{div} \, \mathbf{v}_h \, d\mathbf{x}.$$

This (numerical differentiation) task (as well–known) is an ill-posed problem. To resolve this issue, we choose to minimize the total variation (or TV) functional (subject to the prescribed averages equality constraints) since this functional gives non–oscillatory recovery. An illustration of a TV constrained minimization procedure is shown in Figure 4: a discontinuous (piecewise constant) function is approximated on a locally refined mesh by an $H^1$–conforming finite element function.

In the recovery procedure, we need a second (finite element) mesh $\mathcal{T}_h$, a refinement of the primal (FV or finite element) mesh $\mathcal{T}_H$. We note that the accuracy of the overall scheme is determined by the primal mesh $\mathcal{T}_H$. The TV function recovery reads: Find a finite element function $\mathbf{v}_h$ with minimal total variation

$$\mathbf{J}_{TV}(\mathbf{v}_h) = \int\limits_{\Omega} |\nabla \mathbf{v}_h| \, d\mathbf{x} \mapsto \min,$$

with prescribed integral moments for all $V = V_{n+1} \in \mathcal{T}_H$

$$\int\limits_{V} \varrho \, \mathbf{v}_h \, d\mathbf{x}.$$

In addition to the above (equality) constraints, we impose inequality constraints that represent the non-negativity of the internal energy. To this end, consider the conservation of energy equation (for $T \in \mathcal{T}_h$):

$$\int\limits_{T_{n+1}} \varrho_{n+1} E_{n+1} \, d\mathbf{x} = \int\limits_{T_n} \varrho_n E_n \, d\mathbf{x}_n - \Delta t \int\limits_{\partial T_{n+1}} p_h \mathbf{v}_h \cdot \mathbf{n} \, d\sigma.$$

Since

$$E = e + \frac{1}{2} |\mathbf{v}|^2,$$

and from physical consideration (nonnegative internal energy), we have

$$0 \le \left( \int\limits_{T_{n+1}} \varrho e \, d\mathbf{x} = \right) \int\limits_{T_n} \varrho_n E_n \, d\mathbf{x}_n - \Delta t \int\limits_{\partial T_{n+1}} p_h \mathbf{v}_h \cdot \mathbf{n} \, d\sigma - \frac{1}{2} \int\limits_{T_{n+1}} \varrho_{n+1} \, |\mathbf{v}_h|^2 \, d\mathbf{x}.$$

This is a quadratic inequality constraint for $\mathbf{v}_h = \mathbf{v}_{n+1}$ imposed on any $T = T_{n+1} \in \mathcal{T}_h$ for given $\varrho_{n+1}$ and $p_h$.

A similar somewhat simpler problem can be formulated for $p_h$. Note that the quadratic inequality constraint for $\mathbf{v}_h$ implies (using the E.O.S.) nonnegativity of the average pressure $\overline{p} \equiv \frac{\gamma-1}{|V_{n+1}|} \int\limits_{V_{n+1}} \varrho e \, d\mathbf{x} \ge 0$.

## 3. Implementation of the function recovery based FV schemes

In this section, we summarize in an algorithm form (presented for the lowest order case $\underline{\alpha} = 0$) the main steps needed to implement our FV/DG schemes.

We have a primal (moving) mesh $\mathcal{T}_H$. In the recovery procedures, we need a dynamically constructed mesh $\mathcal{T}_h$ that is a refinement of $\mathcal{T}_H$. With $\mathcal{T}_h$ we associate a finite element space $S_h$ that is $H^1$-conforming. Its vector version will be denoted $\mathbf{S}_h = (S_h)^d$. A typical choice is $S_h$ piecewise linear.

**Algorithm 3.1** (Conservative FV Scheme)**.**

*Let $\{\mathbf{x}_n\}$ be the set of vertices of the primal cells in $\mathcal{T}_H$ at time $t_n$. The algorithm below computes $\mathbf{x}_h$, $\mathbf{v}_h \in \mathbf{S}_h$ and $p_h \in S_h$ by iterations. It also computes the average values $\overline{\mathbf{v}}$ and $\overline{p}$ over the moving primal cells.*

- *To move the mesh, find a finite element function $\mathbf{x}_h \in \mathbf{S}_h$ such that*

$$\|\mathbf{x}_h - (\mathbf{x}_n + \Delta t \, \overline{\mathbf{v}}_n)\|_0^2 + \epsilon \int\limits_{\Omega_n} |\nabla \mathbf{x}_h| \mapsto \min .$$

  *Then, $\mathbf{x}_{n+1}$ equals $\mathbf{x}_h$ restricted to the vertices of $\mathcal{T}_H$ (at $t = t_n$) and defines the vertices of the moved $\mathcal{T}_H$ at time $t = t_{n+1}$. Thus, we can compute the volumes $|V|$ for any cell $V = V_{n+1} \in \mathcal{T}_H$. Hence,*

$$\varrho_{n+1} = \frac{m(V)}{|V_{n+1}|}, \qquad \overline{\mathbf{v}}_{n+1} = \frac{1}{m(V)} \left[ \int\limits_{V_n} \varrho_n \mathbf{v}_n \, d\mathbf{x}_n - \Delta t \int\limits_{V_{n+1}} \nabla p_h \, d\mathbf{x}_{n+1} \right].$$

- *Solve the constrained energy minimization problems for $\mathbf{v}_h \in \mathbf{S}_h$ and $p_h \in S_h$:*

$$\mathbf{J}_{ROF}(\mathbf{v}_h) = \|\mathbf{v}_h - \overline{\mathbf{v}}_{n+1}\|^2_{0,\,\varrho_{n+1}} + \epsilon \int\limits_{\Omega_{n+1}} |\nabla \mathbf{v}_h| \, d\mathbf{x}_{n+1} \mapsto \min,$$

$$J_{ROF}(p_h) = \|p_h - \overline{p}_{n+1}\|_0^2 + \epsilon \int\limits_{\Omega_{n+1}} |\nabla p_h| \, d\mathbf{x}_{n+1} \mapsto \min,$$

*subject to the quadratic inequality constraints for any* $T = T_{n+1} \in \mathcal{T}_h$

$$-\frac{1}{2}\int\limits_{T_{n+1}} \varrho_{n+1}\,|\mathbf{v}_h|^2\,d\mathbf{x} - \Delta t \int\limits_{\partial T_{n+1}} p_h \mathbf{v}_h \cdot \mathbf{n}\,d\sigma + \int\limits_{T_n} \varrho E_n\,d\mathbf{x}_n \geq 0.$$

We note that we have incorporated the equality constraints into the TV functional imposed (approximately) as a penalty. The resulting, Rudin-Osher-Fatemi (or ROF) functional ( [2]), is very popular in noise removal algorithms.

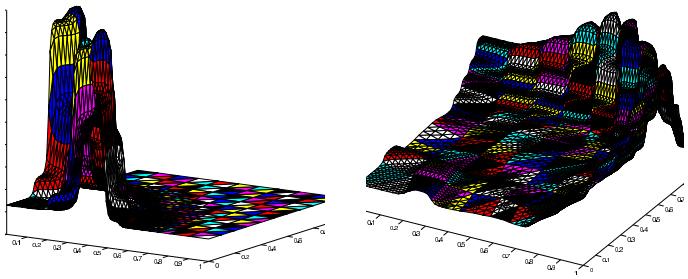

FIGURE 1. Recovered pressure at time $t = 0.2005$ and $t = 0.8005$.

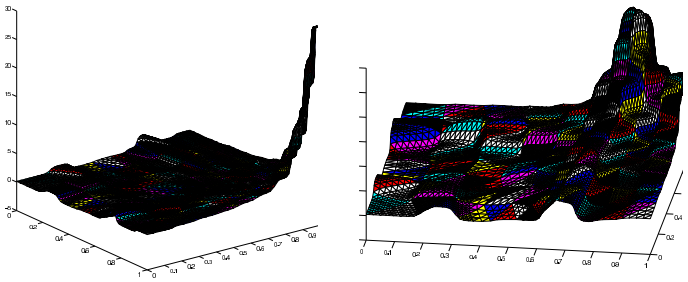

FIGURE 2. Recovered pressure at time $t = 1.0005$ and $t = 1.1005$.

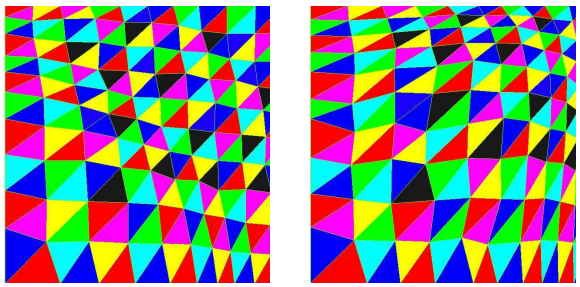

FIGURE 3. Moved mesh at time $t = 0.4005$ and $t = 0.8005$.

The above algorithm contains several inner–outer loops. They can be arranged in a number of ways. For example, starting with some initial approximation for $p_h$ (one possibility is to use an explicit time stepping approximation), we compute the average values $\overline{\mathbf{v}}_{n+1}$ and then solve (approximately) the constrained minimization problem for $\mathbf{v}_h$. Once we have $\mathbf{v}_h$ and $p_h$, we can compute the moments

$$\frac{1}{|V_{n+1}|}\int\limits_{V_{n+1}} \varrho e \, d\mathbf{x} = \frac{1}{|V_{n+1}|}\left[\int\limits_{V_n} \varrho_n E_n \, d\mathbf{x}_n - \Delta t \int\limits_{\partial V_{n+1}} p_h \mathbf{v}_h \cdot \mathbf{n} \, d\sigma - \frac{1}{2}\int\limits_{V_{n+1}} \varrho_{n+1} \, |\mathbf{v}_h|^2 \, d\mathbf{x}\right].$$

From the E.O.S. we can then compute the averages $\overline{p}_{n+1} = \frac{1}{|V_{n+1}|}\int\limits_{V_{n+1}} p_h \, d\mathbf{x}$ and solve the ROF–minimization problem for a new pressure approximation $p_h$. The process can be repeated several times. At every step, we refine the mesh $\mathcal{T}_h$ gradually to capture the possible large gradients of $p_h$ (and $\mathbf{v}_h$). The ROF–minimization problems are linearized using simple Picard approximation coupled with the local mesh refinement of $\mathcal{T}_h$, then the quadratic constrained minimization problems are approximately solved by 1D monotone Gauss–Seidel iterations.

## 4. Numerical illustration

We consider a model test problem posed on the unit square domain $\Omega$. We set at the initial time $t = 0$, $\mathbf{v} = 0$ and $\rho = 1$. Also, the pressure $p$ is zero outside a single volume (square) $V \in \mathcal{T}_H$ and $p$ equals to a constant on $V$ such that $\int\limits_{\Omega} \rho E \, d\mathbf{x} = 1$. We keep $\mathbf{v} \cdot \mathbf{n} = 0$ on $\partial\Omega$ for $t \geq 0$ so that the domain $\Omega$ stays fixed.

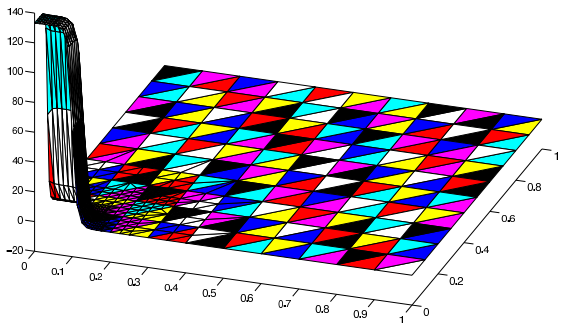


Figure 4. TV recovered pressure at time $t = 0.0005$.

In the figures we show how the shock wave travels from the bottom left corner of $\Omega$, reaches the opposite one and starts coming back. Although the results are only preliminary and not as accurate, the potential of the schemes is clearly

seen. We expect much better results when the higher order moments ($\underline{\alpha} \neq 0$) are incorporated combined with higher order time discretization.

*Acknowledgment.* This work was performed under the auspices of the U.S. Department of Energy by Lawrence Livermore National Laboratory under Contract DE-AC52-07NA27344.

## References

[1] E. Godlewski and P.-A. Raviart, "*Numerical Approximation of Hyperbolic Systems of Conservation Laws,*" Springer series in Applied Mathematical Sciences vol. **118**(1996), Springer-Verlag, New York.

[2] L. Rudin, S. Osher and E. Fatemi, "*Nonlinear total variation based noise removal algorithms,*" Phys. D **60**(1992), pp. 259-268.

[3] P. S. Vassilevski, "*Novel Two-Scale Discretization Schemes for Lagrangian Hydrodynamics,*" Lawrence Livermore National Laboratory Technical Report LLNL-TR-404477, 2008.

## Domain decomposition theory when subdomains are irregular

Olof Widlund

(joint work with Clark R. Dohrmann, Axel Klawonn, Oliver Rheinbach)

In the theory for domain decomposition methods, we have previously often assumed that each subdomain is the union of a small set of coarse shape-regular triangles or tetrahedra. In this study, we discuss recent progress which makes it possible to analyze cases with irregular subdomains such as those provided by mesh partioners.

Our goal is to extend our analytic tools to problems on subdomains that might not even be Lipschitz and to characterize the rates of convergence of our methods in terms of a few, easy to understand, geometric parameters of the subregions. For two dimensions, we have already obtained some best possible results for scalar elliptic and linear elasticity problems: the subdomains should be John or Jones domains and the rate of convergence is determined using the parameters that define such domains and tha of an isoparametric inequality. Progress and three dimensions will also be reported.

New results have also recently been obtained concerning variants of classical two level additive Schwarz preconditioners. Our family of overlapping Schwarz methods borrows and extends coarse spaces from older iterative substructuring methods, i.e. methods based on non-overlapping sudbomains. The local components of these preconditioners, on the other hand, are based on Dirichlet problems defined on a set of overlapping subdomains which cover the original domain.

Our methods are robust even in the presence of large changes, between subdomains, of the materials being modeled in the finite element models. An extra attraction is that our methods can be applied directly to problems where the stiffness matrix is available only in its fully assembled form.

We will also discuss several applications of the new tools. They include new results on almost incompressible elasticity and mixed finite elements using spaces of

discontinuous pressures. We will also touch on recent work on Maxwell's equations in two dimensions.

Our work has been carried out in close collaboration with Clark R. Dohrmann of the Sandia National Laboratories, Albuquerque, NM, and Axel Klawonn and Oliver Rheinbach of the University of Duisburg-Essen, Germany.

## SQP methods for plastictiy

Christian Wieners

The radial return together with a consistent linearization is the standard solution procedure for incremental plasticity. Although this class of algorithm is very general (with variants for a broad variety of plasticity models) and in most cases also efficient and reliable, the convergence analysis is restricted to simple situations. In particular, the standard approach can be reformulated as a semi-smooth Newton method, and—since the radial return is Lipschitz and strongly semi-smooth—we obtain locally quadratic but globally mesh-dependent convergence.

This can be improved by the application of well understood methods in mathematical programming. Algorithms in mathematical programming have a long tradition in computational plasticity, in particular for the solution of local optimization problem for the internal variables. In the last years algorithms of numerical optimization where transferred to the full variational problem of incremental plasticity: semi-smooth Newton methods for a simultaneous approximation of displacement and plastic strain, interior-point algorithms and SQP methods.

In particular SQP methods appear to have a structural advantage: the SQP iterates for the stresses are a minimizing sequence for the dual minimization problem in incremental plasticity, whereas the iterates for the displacements of the radial return method minimize a suitable primal functional. Since the dual problem for the stress is uniformly convex (which is not the case for the primal displacement problem), we expect (and indeed observe in examples) at least asymptotically better convergence for the SQP method. Nevertheless, in the application to perfect plasticity the solution of the quadratic problem in the single SQP step remains difficult and no uniform bounds are available.

In this contribution we present the SQP method for perfect plasticity and for a plasticity model with hardening. Hardening adds some regularity to the quadratic problem in the single SQP step, so that we now can prove global convergence for the semi-smooth Newton method which is used to solve this quadratic minimization problem with linearized constraints.

The new algorithm can be realized by a linearization of the flow rule which then leads to a sequence of linear variational problems with linear inequality constraints. So, the subproblem itself can be realized with a simplified radial return algorithm. This fits perfectly into our framework of parallel finite elements, so that large scale simulations are possible. In addition, this solution method transfers to

more advanced models such as elasto-plastic non-polar models (with appended infinitesimal Cosserat rotations) and to nonlocal plasticity.

### References


[1] C. Wieners, *Distributed point objects. A new concept for parallel finite elements*, in R. Kornhuber, R. Hoppe, J. Périaux, O. Pironneau, O. Widlund, and J. Xu, editors, *Domain Decomposition Methods in Science and Engineering*, volume 40 of *Lecture Notes in Computational Science and Engineering*, Springer-Verlag Berlin (2004) 175–183.

[2] C. Wieners, *Nonlinear solution methods for infinitesimal perfect plasticity*, Z. Angew. Math. Mech. (ZAMM) **87** (2007) 643–660

[3] P. Neff, K. Chelminski, W. Müller, and C. Wieners, *A numerical solution method for an inifinitesimal elasto-plastic cosserat model* Mathematical Models and Methods in Applied Sciences (M3AS) **17** (2007) 1211–1240.

[4] P. Neff, A. Sydow, and C. Wieners, *Numerical approximation of incremental infinitesimal gradient plasticity*, Int. J. Numer. Meth. Eng. (2008), to appear.

[5] C. Wieners, *SQP methods for incremental plasticity with kinematic hardening*, in Distributed point objects. A new concept for parallel finite elements. In D. Reddy, editor, *Theoretical, Modelling and Computational Aspects of Inelastic Media*, Lecture Notes in Computational Science and Engineering, Springer-Verlag Berlin, to appear 2009


## Automated Transformations of PDE Systems

Irad Yavneh, Shmuel Onn, Yossi Gil, Zvika Gutterman

We study an approach for transforming systems of partial differential equations (PDE) in order to obtain new formulations, especially decoupled ones that are more accessible to numerical solution. An algorithm is developed for generating such transformations automatically, using symbolic manipulations employing Groebner bases. The algorithm is implemented using freely available symbolic software. This approach, along with planned developments, will potentially provide a powerful set of tools for handling large systems of partial differential equations.

## Sparse Grids and the exponential representation of functions

Harry Yserentant

Methods that are suitable to approximate high-dimensional functions need to have properties that largely contradict each other. They should first be able to take advantage of smoothness properties like the existence of high-order mixed derivatives and of symmetry properties as they are common in theoretical physics and chemistry. Secondly, they should reproduce products of lower dimensional functions as products of same type. These goals can hardly be reached with methods that are based on linear ansatz spaces. In the talk a construction has been presented that satisfies all these conditions and does basically not suffer from the curse of dimensionality. It is based on the representation of functions in terms of certain excitation operators. These operators form a commutative Banach algebra and can be represented in exponential form.

## Cache oblivious Memory Management for PDE-solvers

Christoph Zenger
(joint work with Michael Bader and Miriam Mehl)

In modern Computer architectures, the gap between the relatively high speed of arithmetic processor units and the relatively low speed of access to memory reduces the efficiency of programs for numerical simulations in an intolerable way, and this situation shall even deteriorate in the future. This is observed especially, if the access to memory addresses jumps in an irregular way, because in this case the cache hierarchy designed to reduce the significance of the problem cannot work properly. In computer science, algorithms working on stacks or tapes play an important role, and, because the access to stacks or tapes stays always local, the problem of memory non-locality is also substantially reduced. We demonstrate that this technique can also be used successfully in scientific computing algorithms. In an introductory example, we analyse an algorithm for matrix multiplication, where the matrices are stored on tapes with a special ordering based on Peano space filling curves. In this algorithm, access to memory moves only from one location to a direct neighbour. Jumps do not occur, which results in a very efficient program execution on modern processor architectures. [BZ, HB]

As a more sophisticated example, we present a computational kernel for an adaptive multilevel solver for elliptic PDEs based on hierarchically refined space tree grids. It can be shown that essentially all data, which grows linearly with the number of unknowns, can be stored on 8 stacks during the execution of the program for a three-dimensional space tree. Thus, access to memory stays strictly local. Among other advantages of the program structure, a dramatic reduction of cache misses is observed in comparison to standard implementations. [GMPZ, MWZ] This advantage would be even more visible, if modern operating systems would support stacks and tapes as basic data structures as they do, for example, for pipes. Moreover, memory modules used for stacks or tapes would not require address calculations, which shows further potential for acceleration by a specialized memory architecture.

### References

[BZ] M. Bader and C. Zenger, Cache oblivious matrix multiplication using an element ordering based on a Peano curve. Linear Algebra and Its Applications 417 (2–3), p. 301–313, 2006.

[HB] A. Heinecke and M. Bader, Parallel matrix multiplication based on space-filling curves on shared memory multicore platforms. In: Proceedings of the 2008 Computing Frontiers Conference and co-located workshops: MAW'08 and WRFT'08, p. 385–392, 2008.

[GMPZ] F. Günther, M. Mehl, M. Pögl, and C. Zenger, A cache-aware algorithm for PDEs on hierarchical data structures based on space-filling curves. SIAM Journal on Scientific Computing 28 (5), pp. 1634–1650, 2006.

[MWZ] M. Mehl, T. Weinzierl, and C. Zenger, A cache-oblivious self-adaptive full multigrid method. Numerical Linear Algebra with Applications 13 (2-3), pp. 275–291, 2006.

*Reporter: Alfio Grillo*

# Participants

**Prof. Dr. Randolph E. Bank**
Dept. of Mathematics
University of California, San Diego
9500 Gilman Drive
La Jolla, CA 92093-0112
USA

**Dr. Steffen Börm**
Max-Planck-Institut für Mathematik
in den Naturwissenschaften
Inselstr. 22 - 26
04103 Leipzig

**Prof. Dr. Folkmar A. Bornemann**
Zentrum Mathematik
Technische Universität München
85747 Garching bei München

**Prof. Dr. Dietrich Braess**
Fakultät für Mathematik
Ruhr-Universität Bochum
Universitätsstr. 150
44801 Bochum

**Prof. Dr. Wolfgang Dahmen**
Institut für Geometrie und
Praktische Mathematik
RWTH Aachen
Templergraben 55
52056 Aachen

**Dr. Robert D. Falgout**
Center of Applied Scientific Computing
Lawrence Livermore National Laboratory
P.O.Box 808, L-561
Livermore, CA 94551
USA

**Dr. Peter Frolkovic**
Department of Mathematics
Faculty of Civil Engineering
Slovak University of Technology
Radlinskeho 11
81368 Bratislava
SLOVAKIA

**Dr. Alfio Grillo**
IWR Technische Simulation
Universität Heidelberg
Im Neuenheimer Feld 368
69120 Heidelberg

**Univ.-Prof. Dr. Gundolf Haase**
Institut für Mathematik und
wissenschaftliches Rechnen
Karl-Franzens-Universität Graz
Heinrichstr. 36
A-8010 Graz

**Prof. Dr. Wolfgang Hackbusch**
Max-Planck-Institut für Mathematik
in den Naturwissenschaften
Inselstr. 22 - 26
04103 Leipzig

**Prof. Dr. Pieter W. Hemker**
Centrum voor Wiskunde en
Informatica
Kruislaan 413
NL-1098 SJ Amsterdam

**Prof. Dr. Ralf Hiptmair**
Seminar für Angewandte Mathematik
ETH-Zentrum
Rämistr. 101
CH-8092 Zürich

**Prof. Dr. Michael Holst**
Dept. of Mathematics
University of California, San Diego
9500 Gilman Drive
La Jolla, CA 92093-0112
USA

**Prof. Dr. Ronald H.W. Hoppe**
Lehrstuhl für Angewandte
Mathematik I
Universität Augsburg
Universitätsstr. 14
86159 Augsburg

**Prof. Dr. Klaus Johannsen**
Bergen Center for Computational Science
Universitet i Bergen
Thormöhlensgt. 55
N-5008 Bergen

**Dr. Boris N. Khoromskij**
Max-Planck-Institut für Mathematik
in den Naturwissenschaften
Inselstr. 22 - 26
04103 Leipzig

**Prof. Dr. Ralf Kornhuber**
Institut für Mathematik II (WE2)
Freie Universität Berlin
Arnimallee 2-6
14195 Berlin

**Prof. Dr. Ulrich Langer**
Institut für Numerische Mathematik
Johannes Kepler Universität Linz
Altenbergerstr.69
A-4040 Linz

**Prof. Dr. Sabine Le Borne**
Dept. of Mathematics
Tennessee Technological University
Cookeville, TN 38505
USA

**Prof. Dr. Volker Mehrmann**
Institut für Mathematik
Technische Universität Berlin
Sekr. MA 4-5
Strasse des 17. Juni 136
10623 Berlin

**Prof. Dr. Arnd Meyer**
Fakultät für Mathematik
TU Chemnitz
Reichenhainer Str. 41
09126 Chemnitz

**Prof. Dr. Zeyao Mo**
Institute of Applied Physics and
Computational Mathematics
P.O.Box 8009
Beijing 100088
P.R.China

**Arne Nägel**
IWR Technische Simulation
Universität Heidelberg
Im Neuenheimer Feld 368
69120 Heidelberg

**Dr. Cornelis Oosterlee**
Faculty of Technical Mathematics
and Informatics
Delft University of Technology
Mekelweg 4
NL-2628 CD Delft

**Prof. Dr. Peter Oswald**
School of Engineering and Science
Jacobs University Bremen
Postfach 750561
28725 Bremen

**Dr. Daniel Peterseim**
Institut für Mathematik
Universität Zürich
Winterthurerstr. 190
CH-8057 Zürich

**Gillian Queisser**
IWR Technische Simulation
Universität Heidelberg
Im Neuenheimer Feld 368
69120 Heidelberg

**Prof. Dr. Arnold Reusken**
Institut für Geometrie und
Praktische Mathematik
RWTH Aachen
Templergraben 55
52062 Aachen

**Prof. Dr. Thomas F. Russell**
Division of Mathematical Sciences
National Science Foundation
4201 Wilson Blvd
Arlington, VA 22230
USA

**Prof. Dr. Volker Schulz**
Fachbereich IV - Mathematik
Numerik - Optimierung, partielle
Differentialgleichungen
Universität Trier
54286 Trier

**Prof. Dr. Rob Stevenson**
Dept. of Mathematics
University of Amsterdam
Plantage Muidergracht 24
NL-1018 TV Amsterdam

**Dr. Klaus Stüben**
Fraunhofer-Institut für
Algorithmen und Wissenschaftliches
Rechnen (SCAI)
Schloss Birlinghoven
53754 Sankt Augustin

**Prof. Dr. Panayot S. Vassilevski**
Center for Applied Scientific Computing
Lawrence Livermore National Laboratory
P.O.Box 808, L-560
Livermore CA 94550
USA

**Prof. Dr. Olof B. Widlund**
Courant Institute of
Mathematical Sciences
New York University
251, Mercer Street
New York, NY 10012-1110
USA

**Prof. Dr. Christian Wieners**
Institut für Angewandte und Numerische
Mathematik
Universität Karlsruhe
Englerstr. 2
76131 Karlsruhe

**Prof. Dr. Gabriel Wittum**
IWR Technische Simulation
Universität Heidelberg
Im Neuenheimer Feld 368
69120 Heidelberg

**Prof. Dr. Barbara Wohlmuth**
Institut für Angewandte Analysis
und Numerische Simulation
Universität Stuttgart
Pfaffenwaldring 57
70569 Stuttgart

**Konstantinos Xylouris**
IWR Technische Simulation
Universität Heidelberg
Im Neuenheimer Feld 368
69120 Heidelberg

**Prof. Dr. Irad Yavneh**
Computer Science Department
TECHNION
Israel Institute of Technology
Haifa 32000
ISRAEL

**Prof. Dr. Harry Yserentant**
Institut für Mathematik
Technische Universität Berlin
Straße des 17. Juni 136
10623 Berlin

**Prof. Dr. Christoph Zenger**
Institut für Informatik
TU München
Boltzmannstr. 3
85748 Garching